Copyright Warning & Restrictions

The copyright law of the United States (Title 17, United States Code) governs the making of photocopies or other reproductions of copyrighted material.

Under certain conditions specified in the law, libraries and archives are authorized to furnish a photocopy or other reproduction. One of these specified conditions is that the photocopy or reproduction is not to be "used for any purpose other than private study, scholarship, or research." If a, user makes a request for, or later uses, a photocopy or reproduction for purposes in excess of "fair use" that user may be liable for copyright infringement,

This institution reserves the right to refuse to accept a copying order if, in its judgment, fulfillment of the order would involve violation of copyright law.

Please Note: The author retains the copyright while the New Jersey Institute of Technology reserves the right to distribute this thesis or dissertation

Printing note: If you do not wish to print this page, then select "Pages from: first page # to: last page #" on the print dialog screen

ABSTRACT

Time Frequency Analysis of Electromyogram During Muscle Fatigue

by

Michelle Rene Davies

Spectral parameters obtained from the surface EMG signal have been used as indicators of fatigue during a sustained contraction. These same parameters have not been tested with the EMG signals obtained from fine wire electrodes. One such parameter is the median frequency which is known to decline with fatigue. A comparison was done between the median frequencies obtained from the surface EMG and those obtained from the fine wire EMG. The median frequencies from both types of electrodes decreased with time, indicating that fine wire electrodes could be used to measure fatigue.

In addition, a new technique, time frequency analysis, was applied to the EMG signal. This technique generates a continuos representation of the changing spectrum of the signal through time. Three types of time frequency distributions were applied to the EMG signal. As predicted, differences existed between the distributions. The amplitude differential from the first time slice of the distribution to the last was the smallest for the STFT distribution. The Wigner-Ville distribution was spread out across the most frequencies. Walls appeared in the Choi-Williams distribution, but otherwise it was the most compressed. All the distributions displayed the expected spectral compression; however, more work is necessary to clarify the results.

TIME FREQUENCY ANALYSIS
OF THE
ELECTROMYOGRAM DURING FATIGUE

by
Michelle Rene Davies

A Thesis
Submitted to the Faculty of
New Jersey Institute of Technology
in Partial Fulfillment of the Requirements for the Degree
Master of Science in Biomedical Engineering

Biomedical Engineering Committee

January 1994

APPROVAL PAGE

Time Frequency Analysis of Electromyogram During Fatigue

Michelle Rene Davies

Dr. Stanley S. Reisman, Thesis Advisor — Date
Professor of Electrical Engineering, New Jersey Institute of Technology

Dr. David Kristol, Committee Member — Date
Director, Biomedical Engineering Program, New Jersey Institute of Technology

Dr. Thomas W. Findley, Committee Member — Date
Director of Research, Kessler Institute for Rehabilitation
Associate Professor, UMDNJ New Jersey Medical School

BIOGRAPHICAL SKETCH

Author: Michelle Rene Davies

Degree: Master of Science in Biomedical Engineering

Date: January 1994

Undergraduate and Graduate Education:

- Master of Science in Biomedical Engineering
  New Jersey Institute of Technology, Newark, NJ, 1994

- Bachelor of Science in Engineering - Electrical Concentration
  LeTourneau University, Longview, Texas, 1990

Major: Biomedical Engineering

This thesis is dedicated to

Larry Davies, my husband, who encouraged and inspired me

and

Larry and Lauana Craig, my parents, who always believed in me.

ACKNOWLEDGEMENT

The author wishes to express her gratitute to her advisor, Dr. Stanley Reisman. He provided more guidance, support and encouragement than was his obligation, but without which this research could not have been completed.

Special thanks to Dr. Lisa Krivikas, who gave the author the opportunity to work with her on her research project and provided valuable medical information.

The author is especially grateful to John Andrews, who took time out of his busy schedule to discuss research with her and to motivate her to ask "why?".

TABLE OF CONTENTS

TABLE OF CONTENTS
(Continued)

LIST OF TABLES

Table **Page**

LIST OF FIGURES

Figure **Page**

Chapter 1

BACKGROUND

1.1 Muscles

The smallest muscular unit that can be controlled by the central nervous system is the motor unit. It consists of all the muscle fibers controlled by one nerve fiber, an α-motoneuron, and the motoneuron. When the motoneuron fires, it triggers the depolarization of the muscle fiber. The depolarization propagates in both directions toward the two ends of the muscle fiber, generating two action potentials (Knaflitz and Balestra, 1991). The final result of an action potential is the contraction of the muscle fiber. The spatial-temporal superposition of the action potentials for all the muscles fibers of one motor unit is called the motor unit action potential. The sequence of motor unit action potentials through time is the motor unit action potential train (Knaflitz and Balestra, 1991). An electrode placed on the skin over the muscle fibers or within the muscle will detect the electromyogram (EMG) signal, which is a summation of the motor unit action potential trains within its vicinity.

1.2 EMG

The electrical manifestation of the neuromuscular activation associated with a contracting muscle is called the EMG signal (Basmajian and DeLuca, 1985). Action potentials, detected by the electrode, can be positive or negative; therefore, the instantaneous sum of motor unit action potentials has both positive and negative components. The resulting EMG signal is very noise-like in appearance. The amplitude of the EMG signal changes depending on the amount of muscle activity. Amplitudes from 50 μV to 1 mV, with frequencies varying from 10 Hz to 3000 Hz, can be seen depending on the type of electrode, the placement of the electrode, and the activity of the muscle (Marieb, 1992).

Figure 1.1 is an example of an EMG signal obtained using surface electrodes.

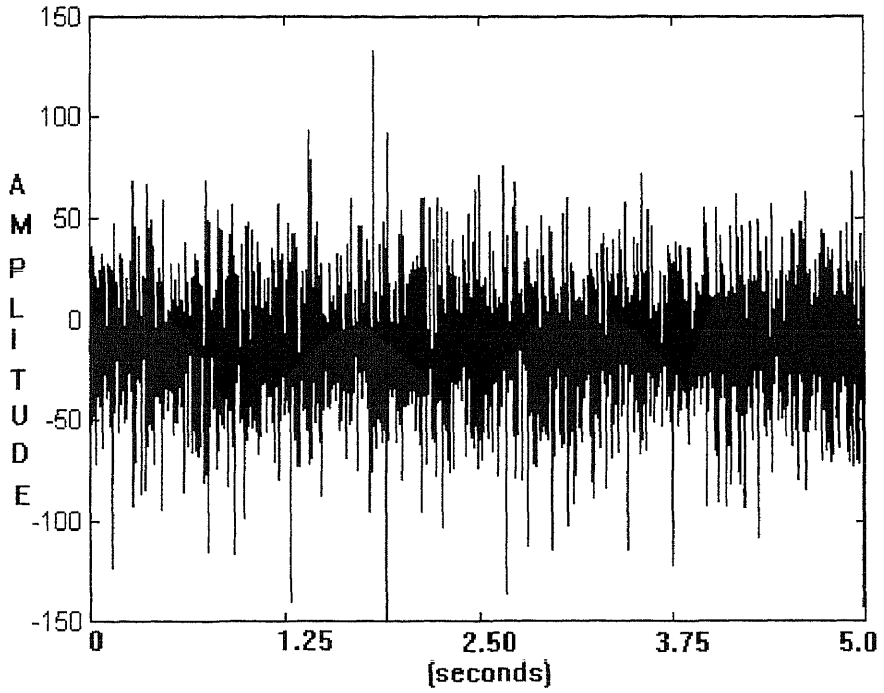

Figure 1.1 EMG signal of biceps brachii muscle obtained using surface electrodes.

1.3 Fatigue

In the past, it was assumed that fatigue was the point in time when a contraction could no longer be held. This definition of fatigue is very subjective. It relies on the subject's desire to hold the contraction. A subject with greater desire will hold the contraction ofr a longer period of time than a subject with less desire. Also, this definition does not correctly relate to the definition of fatigue used in other disciplines such as mechanical or civil engineering. In those disciplines, fatigue is not a distinct point in time but rather a process of weakening through time which ends when failure occurs. The application of this definiation to muscular fatigue, implies that as a contraction is held, the muscle is weakening through time until failure (when the contraction can no longer be maintained) occurs. This definition of muscular fatigue is called physiological fatigue and is

characterized by changes in physiological processes. Sustained muscular contractions produced one type of physiological fatigue. It is associated with the inability to maintain a desired force output, muscular tremor, and localized pain. This fatigue effects only individual muscles or groups of synergistic muscles performing the contraction. Chaffin categorized this type of fatigue as localized muscular fatigue (Basmajian, DeLuca, 1985).

An example of the changes in physiological processes during fatigue is the accumulation of lactic acid. Under normal conditions (non-fatiguing), glucose in the muscle cell is broken down to pyruvic acid and nicotinanide adenine dinucleotide reduced (NADH) to produce adenosine triphosphate (ATP). Chemical energy for use in body cells is stored and released by ATP (Marieb, 1992). ATP is necessary for effective muscle contraction. During long contractions, the delivery of oxygen and glucose to the muscle slows down. The NADH, which under normal conditions would react with oxygen, now converts pyruvic acid to lactic acid. As lactic acid accumulates, the muscle pH drops and the production of ATP is limited. Muscle fatigue begins when ATP is being used faster than it is being produced (Marieb, 1992). Piper, in 1912, was the first to show that the frequency components of the surface EMG signal decrease when a contraction is sustained (Basmajian and DeLuca, 1985).

1.4 Spectral Analysis of EMG Signal

Spectral analysis is a process that begins by transforming a signal from the time domain to the frequency domain. Periodic functions can be represented as a sum of sines and cosines at a fundamental frequency and its harmonics. This sum is called a Fourier series. When a function is non-periodic, components may be present at all frequencies. The Fourier series is expanded to a Fourier Transform to accommodate non-periodic functions. Using Fourier transform techniques, the frequency components of the non-periodic function are found.

A plot of the frequency components is the frequency spectrum. The frequency

spectrum shows the distribution of energy versus frequency for the original signal. By squaring the amplitude of the frequency spectrum, the power density spectrum (PDS) is produced (see Figure 1.2).

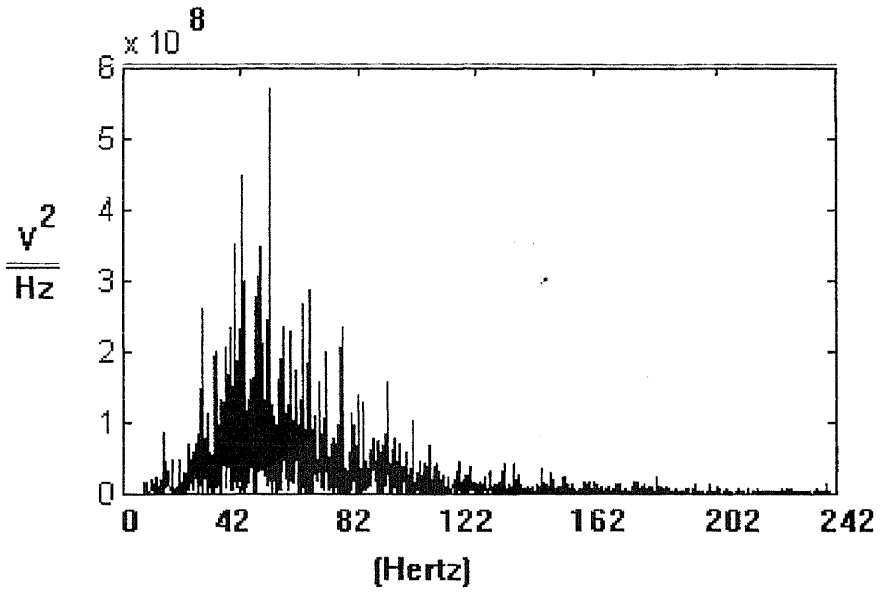

Figure 1.2 A PDS of 5 seconds of surface EMG signal from the biceps brachii.

The theory for applying the Fourier transform to a signal is based on the assumption that the signal exists for all time. When the Fourier transform is applied to a real signal, that begins and ends at a finite time, the spectrum produced differs from the theoretically expected spectrum. For example, the spectrum of a 100 Hz sine wave should simply be a spike at 100 Hz. In reality, the spectrum is shaped in the form of (sin ω)/ω around 100 Hz with side lobes attenuating out from the main lobe (see Figure 1.3).

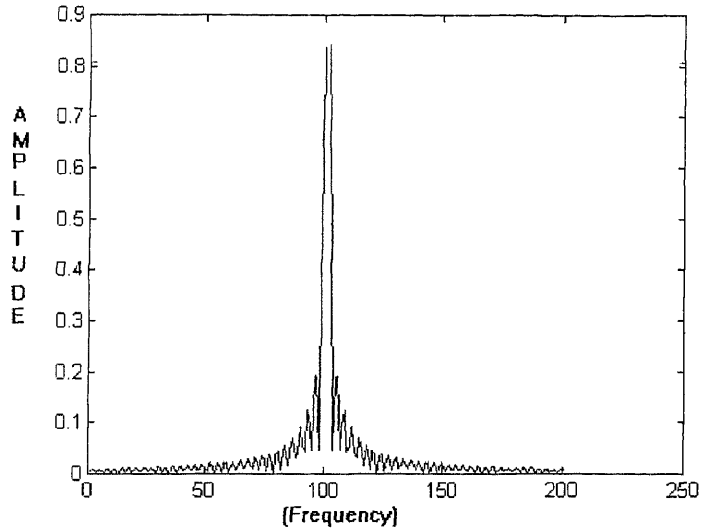

Figure 1.3 Spectrum of a sine wave at 100 Hz, with main lobe and side lobes.

Various windows were developed to attempt to narrow the main lobe and decrease the attenuation of the side lobes. Instead of applying the Fourier transform directly to the desired portion of the signal, the desired portion of the signal is tapered off at the beginning and end by multiplying the signal by a window. The majority of windows developed increase the width of the main lobe, but decrease the attenuation of the side lobes. One type of a window is the hanning window, shown in Figure 1.4.

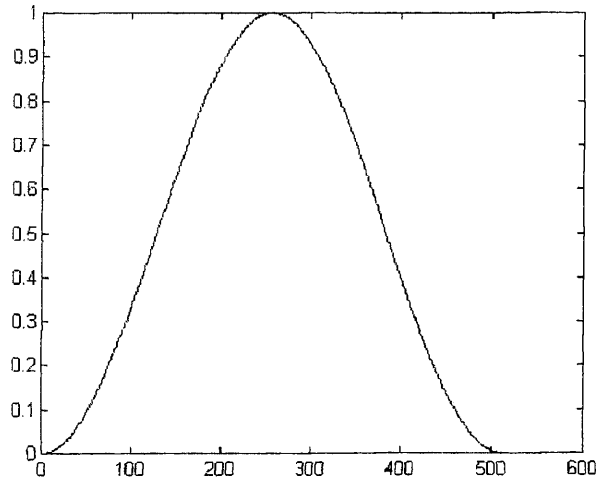

Figure 1.4 Hanning Window.

If the Fourier transform is applied to consecutive time sections of the original EMG signal, multiple power density spectrums will be produced. The power density spectrum of the surface myoelectric signal compresses towards the lower frequencies during a sustained muscle contraction (DeLuca, Sabbahi, Stulen, and Bilotto, 1983). Muscle fatigue during a sustained muscle contraction is very complex and therefore the spectral shift can not reflect the complete muscle fatigue process (Hagg, 1991).

One of the factors affecting this compression of spectral frequency distribution is the muscle fiber conduction velocity. A linear, nonproportional relationship exists between the decay of the muscle fiber conduction velocity and the compression of the PDS to lower frequencies (Linssen et. al., 1993). This compression towards lower frequencies can be quantified. Many parameters values have been utilized, but the median and mean frequencies have been found to be the most reliable. In 1981, the effect of noise on the mean and median frequency was tested by adding white noise to a desired signal (Stulen and DeLuca). They plotted the percentage error in median and mean frequencies versus signal-to-ratio. The percent error for the median frequency was less than the percent error for the mean frequency. When noise is present, the median frequency is a better estimate than the mean frequency (DeLuca, Sabbahi, Stulen, and Bilotto, 1983).

The mean frequency is defined as the average frequency of the PDS. It is found using the following calculation:

$$f_{mean} = \frac{\sum f_i A_i}{\sum A_i} \qquad (1.1)$$

where f_i is the frequency and A_i is the amplitude at that frequency.

The mean power frequency is influenced by the duration of the motor unit action potential, the number of active motor units, and the motor unit firing frequencies. Other factors altering the slope of the PDS are force level, muscle fatigue, muscle and skin temperature, muscle length, distribution of muscle fiber type, skin and tissue impedance,

and electrode properties (Daanen et al., 1990). Daanen et al., in 1990, attempted to control as many factors as possible to verify the reliability of the mean power frequency as an indicator of muscle fatigue. This reported that interindividual subject differences in mean power frequency were large. Differences in the properties of motor unit, muscle fiber type, skin and tissue impedance and localization of the electrodes accounted for the differences in mean power frequency (Daanen et al., 1990). Although intersubject differences exist, intrasubject differences were low. Daanen et.al. concluded that the mean power frequency of the surface EMG is reliable for EMG recording repeated at intervals of several days.

The median frequency is the frequency at which the area of the PDS is divided into two equal portions. It is found using the following calculation:

$$f_{median} = \frac{1}{2}\sum f_i A_i \qquad (1.2)$$

where f_i is the frequency and A_i is the amplitude at that frequency.

Researchers at the Neuromuscular Research Laboratory in Boston investigated the behavior of the median frequency during sustained isometric contractions. They observed that the median frequency decreased as the contraction time progressed. The rate of decrease was higher when the contraction force was higher (DeLuca et al., 1983). DeLuca et al. also showed the measurement of the median frequency to be consistent from day to day.

We have performed a comparison of mean and median frequency calculations for our experimental data and the results appear in Chapter 3.

1.5 Time-Frequency Analysis

Time-frequency techniques are used to analyze signals where the frequency content of the signal changes with time, as is the case with muscle fatigue. In a traditional

frequency spectrum, the spectrum shows all the frequencies present in the signal, but does not indicate when in time and for how much time the frequencies are present. A time-frequency distribution shows at what instants in time those frequencies are present. Time-frequency analysis uses the entire signal and applies the Fourier transform to overlapping sections in time to develop a joint density function that is dependent on both time and frequency. The notation for time frequency analysis used in this paper is:

$s(t)$ - original time signal

$S(w)$ - Fourier transform of original time signal

$P(t,w)$ - time-frequency distribution

$S_t(f)$ - Short Time Fourier Transform distribution

$P_W(t,f)$ - Wigner-Ville distribution

$P_{ch}(t,w)$ - Choi-Williams distribution.

There are eleven desirable properties for any time-frequency distribution: (Amin, Cohen and Williams, 1993)

1. Non negativity

   A density represents a fraction of the components within a certain range; therefore, it should not be negative.

2. Realness

   The density should be real.

3. Time Shift

   When the original signal is translated by a specific time, the whole distribution should also be translated by that time.

4. Frequency Shift

   When the original signal is translated by a specific frequency, the whole distribution should be shifted in frequency by the same frequency.

5. Time Marginal

   The individual time density should be satisfied.

$$\int P(t,w)dw = P_1(t) = |s(t)|^2 \quad (1.3)$$

where $P_1(t)$ is the time marginal.

6. Frequency Marginal

   The individual frequency density should be satisfied.

$$\int P(t,w)dt = P_2(w) = |S(w)|^2 \quad (1.4)$$

   where $P_2(w)$ is the frequency marginal.

7. Instantaneous Frequency

   The frequency in the distribution at a certain time should be the actual frequency of the original signal at that time. This should be true for all frequencies and all time.

8. Group Delay

   The time in the distribution at a certain frequency should be the actual time of the original signal at that frequency.

9. Time Support

   Signals are finite and therefore have a definite beginning before which they are zero and a definite ending after which they are zero. The joint density spectrum should be zero before and after the signal and at any place within the signal that the signal is zero.

10. Frequency Support

    Frequency support is comparable to time support. If the signal is bandlimited, the joint density should be zero outside the band.

11. Reduced Interference

    The distribution should not contain cross terms between frequency components. For a multicomponent signal, the spectrum of each signal should be clearly seen and nothing else.

A common type of time frequency distribution is the Short-Time Fourier Spectrum (STFT). This technique utilizes the basic definition of time-frequency. If

time-frequency distributions look at the frequencies that exist during a certain time section of a signal, then one way to generate this distribution is to take a short time portion of the signal, apply the Fourier transform to it, and proceed to the next time section. At each time a different spectrum is obtained and the totality of these spectra is a time frequency distribution (Amin, Cohen and Williams, 1993). The equation representing this spectrum is:

$$S_t(f) = \int_{-\infty}^{\infty} e^{-j2\pi f\tau} S(\tau) d\tau \quad \text{or} \tag{1.5}$$

$$S_t(f) = \int_{-\infty}^{\infty} e^{-j2\pi f\tau} s(\tau) h(t-\tau) d\tau \text{ when a window is used.} \tag{1.6}$$

The STFT satisfies only four of the desired time frequency properties as listed above. The time and frequency marginals are two of the properties not satisfied. They are not met because the windowing of the STFT changes the characteristics of the original signal. $P_1(t)$ and $P_2(w)$ would approach $|s(t)|^2$ and $|S(w)|^2$ respectively, as required (see Table 1.1) if the windows in the respective domains were narrowed. Both windows cannot be narrowed simultaneously; therefore, the marginals cannot be satisfied (Amin, Cohen and Williams, 1993). Narrowing the window in time yields a poor frequency resolution, while a high frequency resolution is accompanied by a poor time resolution. In general, the STFT distribution works well unless there are very rapid fluctuations in the original signal (Amin, Cohen and Williams, 1993).

The other time frequency distributions are all of the same form, consisting of a kernel and the symmetrical ambiguity function. The general formula for these distributions is:

$$P(t,w) = \frac{1}{4\pi^2} \iiint e^{-j\theta t - j\tau w + j\theta u} \phi(\theta,\tau) s^*(u - \tfrac{1}{2}\tau) s(u + \tfrac{1}{2}\tau) du d\tau d\theta \tag{1.7}$$

Within this formula, the symmetrical ambiguity function is:

$$\chi_s(\theta,\tau) = \int s^*(u - \tfrac{1}{2}\tau) e^{-j\theta u} s(u + \tfrac{1}{2}\tau) du \tag{1.8}$$

while the kernel is represented by $\phi(\theta,\tau)$. For this paper, the equation was rearranged

slightly:

$$\bar{P}(t,w)=\frac{1}{4\pi^2}\int\int e^{-j\tau w}r(u-t,\tau)\,s^*(u-\tfrac{1}{2}\tau)s(u+\tfrac{1}{2}\tau)dud\tau \qquad (1.9)$$

$$r(u,\tau)=\int e^{-j\theta u}\phi(\theta,\tau)d\theta \qquad (1.10)$$

The kernel is the portion of the distribution which changes from one distribution to another. The kernel, therefore, defines which distribution is being used.

The major advantage of defining distribution equations in terms of a kernel is that the properties of the distribution can be determined using only the kernel; the complete distribution equation is not needed.

For the Wigner-Ville distribution, the kernel is one. Essentially the Wigner-Ville distribution is the double Fourier transform of the symmetrical ambiguity function. (Amin, Cohen and Williams, 1993) The equation for this distribution is:

$$P_w(t,f)=\int_{-\infty}^{\infty}e^{-j2\pi f\tau}s^*\left(t-\tfrac{1}{2}\tau\right)s\left(t+\tfrac{1}{2}\tau\right)d\tau \qquad (1.11)$$

The Wigner-Ville distribution satisfies all but two of the desired properties. First, the joint density spectrum produced may be negative. However, this is the case for all distributions except the STFT. The second property it does not meet is of more significance. The joint density spectrum is very noisy. When the original signal is the sum of two or more signals, cross terms are produced:

$$W_{12}(t,w)\equiv\frac{1}{2\pi}\int s_1^*(t-\frac{1}{2}\tau)\,s_2(t+\frac{1}{2}\tau)e^{-j\tau w}d\tau \qquad (1.12)$$

where W_{12} represents the cross term.

The distribution, including the cross terms, will not satisfy property 11. The Wigner-Ville distribution displays very good localization properties, it is generally concentrated around the instantaneous frequency of the signal. However, when the signal evaluated is a multi-component signal, it displays the components of the individual frequencies, but it also displays the cross terms which are spurious (Amin, Cohen and Williams, 1993).

For example, an original signal of a chirp (a sine wave whose frequency increases

linearly) plus a sine wave with a sinusoidally varying frequency was evaluated. The Wigner-Ville distribution for this signal is shown in Figure 1.5. The higher frequency portion of the Wigner-Ville distribution represents the chirp. The lower frequency portion represents the sine wave whose frequency varies as a sine wave. The portion between the two is cross terms and does not represent the frequency components of the original signal.

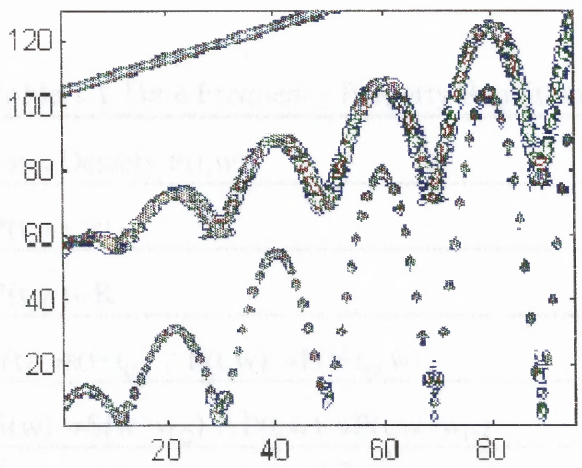

Figure 1.5 Wigner-Ville distribution of a chirp plus a sine wave with sinusoidally varying frequency.

A window is usually added to the Wigner-Ville distribution. This is done for the same reasons a window is added to traditional spectral analysis, the finite nature of the data. The window may suppress certain artifacts, but may also destroy some of the good properties of the Wigner-Ville distribution.

The third distribution used was the Choi-Williams distribution. The Choi-Williams is an example of a reduced interference distribution. The kernel for this distribution is:

$$\phi(\theta,\tau) = e^{\frac{\theta^2\tau^2}{2}} \tag{1.13}$$

The joint density spectrum is then defined as follows:

$$P_{cw}(t,w)=\frac{1}{4\pi^{3/2}}\int\int\frac{1}{\sqrt{\tau^2/\sigma}}e^{-\frac{(u-t)^2}{4\tau^2/\sigma}}e^{-j\tau w}s^*(u-\tfrac{1}{2}\tau)s(u+\tfrac{1}{2}\tau)dud\tau \qquad (1.14)$$

Although the Choi-Williams distribution does not satisfy properties 9 and 10, it does satisfy property 11, reduced interference.

Table 1.1 lists the requirements of each property on the joint density function and the kernel.

Table 1.1 Time Frequency Property Requirements

Property	Joint Density P(t,w)	Kernel $\phi(\theta,\tau)$
1	$P(t,w) \geq 0$	
2	$P(t,w) \in R$	$\phi(\theta,\tau) = \phi^*(-\theta,-\tau)$
3	$s(t) \rightarrow s(t+t_0) \therefore P(t,w) \rightarrow P(t+t_0,w)$	ϕ independ. of time
4	$S(w) \rightarrow S(w+w_0) \therefore P(t,w) \rightarrow P(t,w+w_0)$	ϕ independ. of freq.
5	$\int P(t,w)dw = P_1(t) = \lvert s(t)\rvert^2$	$\phi(\theta,0) = 0$
6	$\int P(t,w)dt = P_2(t) = \lvert S(w)\rvert^2$	$\phi(0,\tau) = 1$
7	$\frac{\int w\,P_t(t,w)dw}{\int P_t(t,w)dw} = w_i(t)$	$\phi(0,\tau) = 1;$ $\left.\frac{\partial\phi(\theta,\tau)}{\partial\theta}\right\rvert_{\tau=0} = 0$
8	$\frac{\int t\,P_t(t,w)dt}{\int P_t(t,w)dt} = t_g(w)$	$\phi(\theta,0) = 0;$ $\left.\frac{\partial\phi(\theta,\tau)}{\partial t}\right\rvert_{\theta=0} = 0$
9	$f(t) = 0$ for $\lvert t\rvert > t_c \Rightarrow P_t(t,w) = 0$ for $\lvert t\rvert > t_c$	$\int \phi(\theta,\tau)e^{-j\theta t}d\theta = 0$ for $\lvert\tau\rvert < 2\lvert t\rvert$
10	$F(w) = 0$ for $\lvert w\rvert > w_c \Rightarrow P_t(t,w) = 0$ for $\lvert w\rvert > w_c$	$\int \phi(\theta,\tau)e^{-j\tau w}d\tau = 0$ for $\lvert\theta\rvert < 2\lvert w\rvert$
11	no cross terms should be present	$\phi(\theta,\tau)$ is a 2D low pass filter

Table 1.2 shows a summary of the properties that are satisfied by the three distributions utilized.

Table 1.2 Time Frequency Properties Satisfied by three distributions

P(t,w)	1	2	3	4	5	6	7	8	9	10	11
STFT	√	√	√	√							
Wigner		√	√	√	√	√	√	√	√	√	
Choi		√	√	√	√	√	√	√			√

1.6 Scope of Thesis

Two of the medical residents at Kessler Institute for Rehabilitation had set up a project to determine if the power spectrum obtained from fine wire electrodes could be used as an indication of muscle fatigue in the same manner that surface electrodes were used. Many technical problems were encountered. The author was requested to join the project to provide technical insight. The hardware for data collection was set up, along with the hardware necessary for analog-to-digital conversion. Software was written to obtain the requested spectral parameters and then the data was analyzed.

The data used in this project is only a small portion of the data collected for the original project; however, some conclusions were drawn regarding the fine wire EMG spectrum median frequency as a indicator of fatigue.

For the project developed by the residents, traditional spectral analysis methods were used as indications of muscle fatigue. This technique analyzes a portion of the original signal completely before proceeding to the next section. To obtain a more complete frequency representation of the entire signal, time frequency analysis techniques were incorporated into the project. Time frequency analysis evaluates the whole signal as one unit.

1.6.1 Goals

Automated Data Collection

The Dantec Counterpoint only permitted spectral analysis of one channel of EMG signal. To correctly compare the decrease of the fine wire EMG median frequency to the decrease of the surface median frequency, the two channels needed to be obtained simultaneously. Another program on the Counterpoint, the EMG oscilloscope program, allowed simultaneous collection of two channels, but did not process the EMG signal. A protocol was developed to acquire the EMG signals from the Dantec Counterpoint to a data acquisition computer where signal processing would take place.

Computerized Analysis of Data

The software was written to obtain the spectral analysis of the EMG signal and to calculate the median frequencies of the spectra.

Analyzed Data

Although the data from only 5 subjects was evaluated for this thesis paper, data was collected from fifteen subjects, two days for each subject, 3 trials a day. The data from all fifteen subjects was analyzed for the original ongoing project studying fine wire versus surface EMG.

Time Frequency Analysis

As the decrease in median frequency shows, the frequency content of the EMG signal changes as the muscle fatigues. Time frequency techniques were developed to analyze signals whose frequency contents change with time. Applying time frequency techniques to the EMG signal during muscle fatigue may add information that was not available using the traditional spectral analysis techniques.

1.6.2 My Contribution

Spectral Analysis

The interfacing between the Dantec Counterpoint and the data acquisition computer was set up. It was designed in such a way that physicians at Kessler Institute for Rehabilitation desiring to study muscle fatigue more can easily connect the equipment to obtain the desired results.

Computer analysis of two channels of EMG was automated, so median frequencies can be readily and easily obtained.

Time Frequency Analysis

Time frequency techniques had never before been used in the Research Lab at Kessler Institute for Rehabilitation. The software had to be developed, and the programs for the STFT and the Wigner-Ville distribution had to be modified for varying applications in the lab, including EMG analysis and ECG analysis. A program for the general kernel distributions was written. It needed only the input of a kernel to distinguish between distributions (produce different distributions). A program was written to produce the Choi-Williams kernel. This kernel was then used with the general distribution program to generate the Choi-Williams distribution.

Time frequency techniques have not previously been applied to EMG signals. All parameters necessary for time frequency techniques had to be chosen: appropriate FFT lengths, number of points skipped, number of time slices, etc.

The time frequency techniques were then applied to signals with known spectra to visualize the differences between the distributions and better understand the distributions. This analysis showed that the STFT produced a wide time-frequency distribution, and the Wigner-Ville distribution contained cross terms.

EMG data, from both fine wire and surface electrodes, was then analyzed using

the time frequency techniques. The distributions produced were very complex and difficult to interpret, but the spectral compression was represented graphically.

CHAPTER 2

METHODS

2.1 Experimental Setup

Fifteen healthy male subjects between the ages of 28 and 38 were tested. Each subject came to two testing sessions with at least one week between sessions. At each of these sessions, fine wire and surface electrodes were used to record the EMG signal of the biceps brachii during an isometric contraction.

2.1.1 Placement of Electrodes

The fine wire electrode was inserted midway between the tendon of the dominant arm and the innervation point of the biceps brachii. The innervation point was estimated to be the peak of the biceps muscle (DeLagi p.66). The midway point for each subject was measured so that electrode placement could be adequately duplicated at subsequent sessions. After insertion, the area around the fine wire electrode was massaged to help the barbs lodge into the muscle. The subject then performed a few isometric contractions to further stabilize the fine wire electrode.

A bipolar bar electrode, Teca 922-6030-1, was placed on the biceps muscle with the active electrode next to the fine wire insertion point. The reference electrode was distal to the active electrode along the midline of the muscle belly in the direction of the muscle fibers.

2.1.2 Muscle Contraction

The subject's dominant arm was put in a wrist splint to lessen the confounding muscle contraction created by wrist flexion. The subjects stood with the arm in a position of 45° elbow flexion, zero degrees shoulder flexion, forearm supinated and wrist extended. The

weight which the subject was requested to hold was based on the subject's maximum voluntary contraction (MVC). The protocol for obtaining the MVC is as follows: have the subject hold the greatest weight he is capable of holding in the test position for 5 seconds without contractile fatigue. Once the MVC was found, a dumbbell between 25% and 35% of the MVC was handed to the subject who was requested to hold it for 100 seconds in an isometric contraction or until contractile fatigue occurred, whichever was first. The subject performed 3 trials per testing session with a five-minute rest period between successive trials. It has been shown that the median frequency recovers essentially five minutes after the contraction is finished (DeLuca et al., 1983).

2.2 Data Analysis

2.2.1 Data Acquisition

During the 100 second contraction, the raw EMG signals from the fine wire electrode and surface electrode were collected simultaneously by a Dantec Counterpoint. The EMG oscilloscope program on the Dantec was selected because it was the only program on the Counterpoint that would allow simultaneous collection from two channels. The following settings were used: sweep speed 50ms/div, sensitivity 2 mV/div. These settings were important, because the output from the Counterpoint is a direct representation of the EMG signal seen on the Counterpoint screen. If all of the EMG signal (with regards to amplitude, not length) was not seen on the screen, the complete signal would not be sent to the data acquisition computer.

A 286 computer was connected to the Dantec Counterpoint at the Amp./Ext. In/Out terminal on the Dantec. Output on this terminal consists of analog amplifier signals from the four channels (Dantec). The acquisition computer had a Keithley Metrabyte Das-16 analog and digital interface board installed. The analog input was set

for ± five volts. The software program used to control the data acquisition was Streamer by Keithley, version 3.25. The protocol for the data acquisition is in Appendix A.

2.2.2 Spectral Analysis

The 100 seconds of EMG signal was divided into 20 sections, each of which contained 5 seconds of the trial. Each five second section contained both fine wire and surface EMG data. The data was then entered into SPlus. SPlus is a data analysis software package that includes modern statistical techniques and permits writing of custom SPlus programs. It was developed at AT&T. Using SPlus, the FFT was applied separately to each five second section of fine wire and then surface EMG data. This resulted in 40 power density spectra (PDS), twenty for the fine wire data and twenty for the surface data. The median frequency of each of the 40 PDSs was then calculated. See Appendix B for details on programming.

The forty median frequencies obtained in SPlus were entered in an Excel spreadsheet where they could be easily manipulated. Excel is a spreadsheet software package by Microsoft. The normalized median frequencies were calculated to compare the decline in median frequencies of the fine wire data to the decline in median frequencies of the surface data over the 100 second contraction.

A linear least squares fit was applied to the normalized median frequencies versus time. The slope, y-intercept, and correlation coefficient were obtained for the line. Those values were then used to compare the relative decline of the fine wire and surface data.

2.2.3 Time Frequency Analysis

The ASCII files, containing the entire EMG signal, were loaded into Matlab, where they were analyzed using time-frequency analysis techniques. Matlab is an interactive software package developed for scientific and engineering numeric computations. It

integrates numerical analysis, matrix computation, signal processing and graphics. To reduce the time necessary to apply the time frequency distributions a more compact signal was needed. The signal needed to be compacted without violating the sampling theorem, which states that the sampling rate must be 2 times the highest frequency present in the signal. For the fine wire data, the highest frequency was assumed to be 1000 Hz, so a sampling rate of 2000 Hz is sufficient. The sampling rate used for the data collection was 4000 Hz,; therefore, the fine wire data could be decimated by 2. The highest frequency present in the surface EMG signal according to Basmajian and DeLuca (1985) is 200 Hz. A sampling rate of 400 Hz is adequate for the surface data, so the original data was decimated by 10.

Three separate time frequency distributions were used in this analysis portion: the Short Time Fourier Transform, the Wigner-Ville distribution and the Choi-Williams distribution.

Chapter 3

RESULTS

3.1 Prelimanary Results

3.1.1 Dantec Mean Frequency Versus Calculated Mean Frequency

The project as originally developed by the residents used the Dantec Counterpoint Power Spectrum program to calculate the mean frequency of one channel of EMG signal. The restriction of this program was that it allowed the output of only the channel evaluated. To compare the spectral parameters of the fine wire EMG signal to those of the surface EMG signal, an output of two channels was needed. Also, it was necessary to compare the mean frequencies found using the developed software program to the values calculated by the Counterpoint. The one channel output from the Counterpoint was sent to a data acquistion computer and then to an analysis computer, where the mean frequencies were evaluated using SPlus. These mean frequencies were compared with the mean frequencies calculated by the Counterpoint Power Spectrum program to verify that the programs were working similarly.

The comparison showed that the mean frequencies were not exactly the same (see Figure 3.1 for an example from one set of data). The major reason for this is that the methods used to obtain the power density spectrum were not exactly the same. The Counterpoint used only the portion of the EMG signal shown on the screen (50ms/div * 10 div = 0.5 secs). The Counterpoint then used a series of 20 sliding windows averaged together to calculate the PDS. The SPlus program calculated the PDS from a 5 second portion of the EMG signal, and no averaging or sliding windows were used. Although the mean frequency values are different, they both decrease with time, as is expected with fatigue, and when normalized, the values are very similar. Therefore, it was acceptable to use the mean frequency generated by the SPlus for the rest of the project.

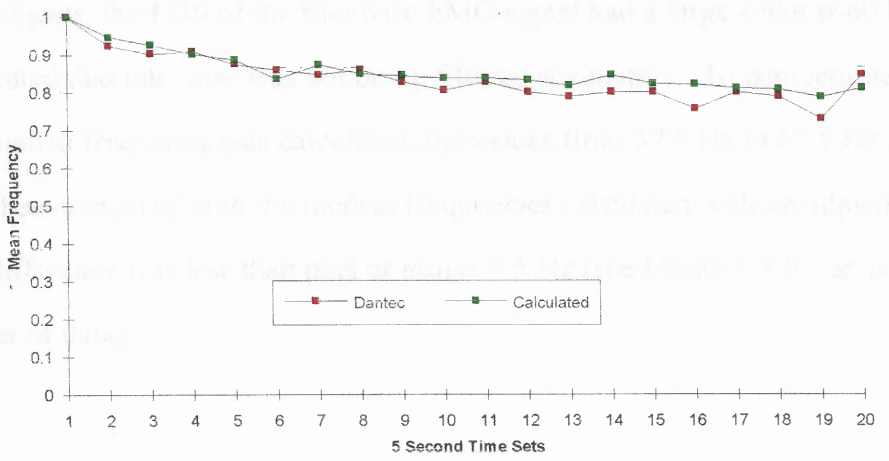

Figure 3.1 Normalized Dantec and Calculated Mean Frequencies

3.1.2 Mean Versus Median Frequency

As stated in Chapter 1, the median frequency is less sensitive to noise than the mean frequency. Both values were calculated for several sets of preliminary data. The absolute values were not the same. Figure 3.2 shows that, when normalized, the values are very similar and have a similar slope. Therefore, median frequencies were used in this project instead of mean frequencies.

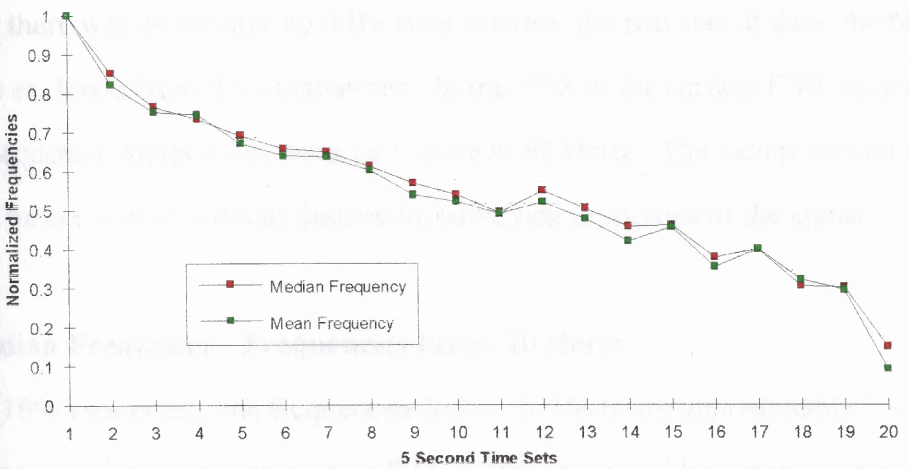

Figure 3.2 Mean and Median Frequencies for one set of data

3.1.3 Median Frequency - 60 Hertz

For some subjects, the PDS of the fine wire EMG signal had a large spike at 60 Hertz, which indicated that the noise was not being filtered adequately. To compensate for this, when the median frequency was calculated, the values from 57.5 Hz to 62.5 Hz were set to zero. When compared with the median frequencies calculated without adjusting for noise, the difference was less than plus or minus 0.5 Hz (see Figure 3.3 for an example from one set of data).

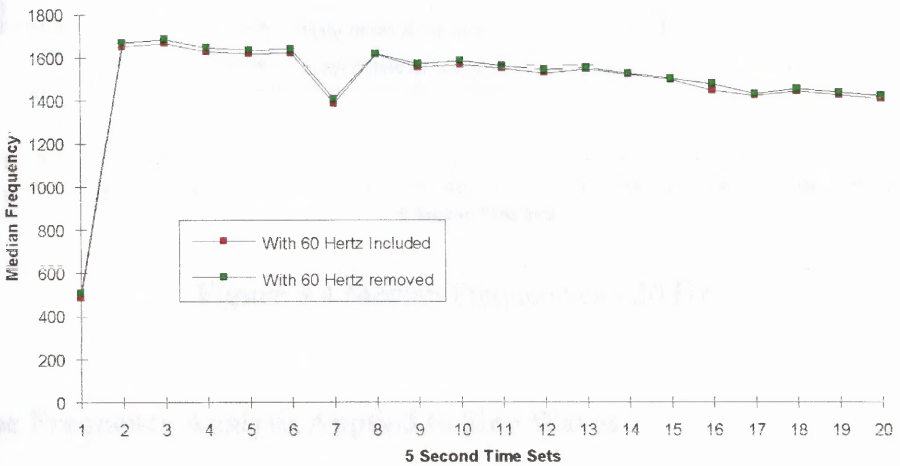

Figure 3.3 Median Frequencies - 60 Hz

Although there was essentially no difference between the two sets of data, the 60 Hertz noise was excluded from the calculations. In the PDS of the surface EMG signal, the normal frequency components were very close to 60 Hertz. The values around 60 Hertz could not be set to zero without destroying some real properties of the signal.

3.1.4 Median Frequency - Frequencies below 20 Hertz

DeLuca (1993) states that the frequencies below 20 Hertz are unpredictable. A comparison was done between median frequencies calculated beginning at zero Hertz and median frequencies calculated beginning at 20 Hertz. Figure 3.4 demonstrates that the values were slightly higher when the frequencies below 20 Hertz were excluded.

However, the normalized values were basically the same. Therefore, for the final results, the frequencies below 20 Hertz were not included in the median frequency calculation.

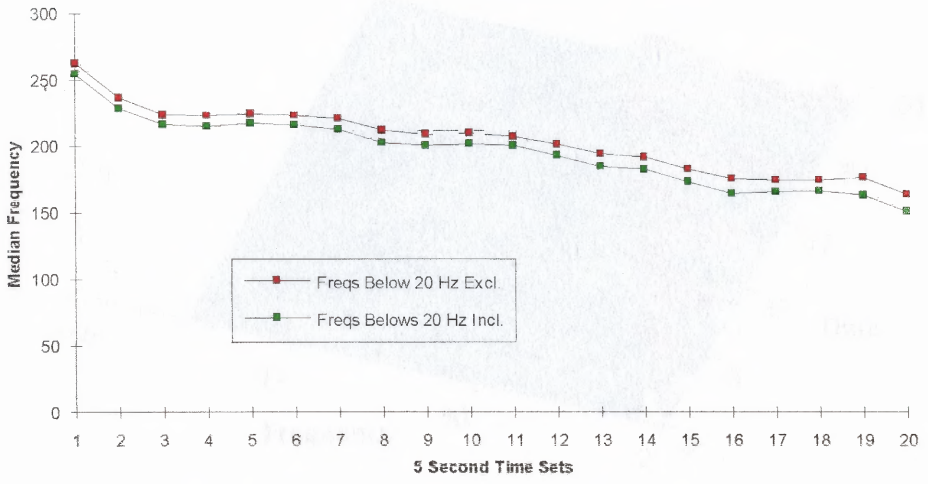

Figure 3.4 Median Frequencies - 20 Hz

3.1.5 Time Frequency Analysis Applied to Sine Waves

The advantages and disadvantages of the three time frequency distributions are more clearly seen when applied to signals with known spectra. The first test signal was a sine wave with sinusoidally varying frequency. All time frequency distributions have the time axis numbers representing the time slice and the frequency axis numbers representing the FFT index. The results are shown in Figure 3.5.

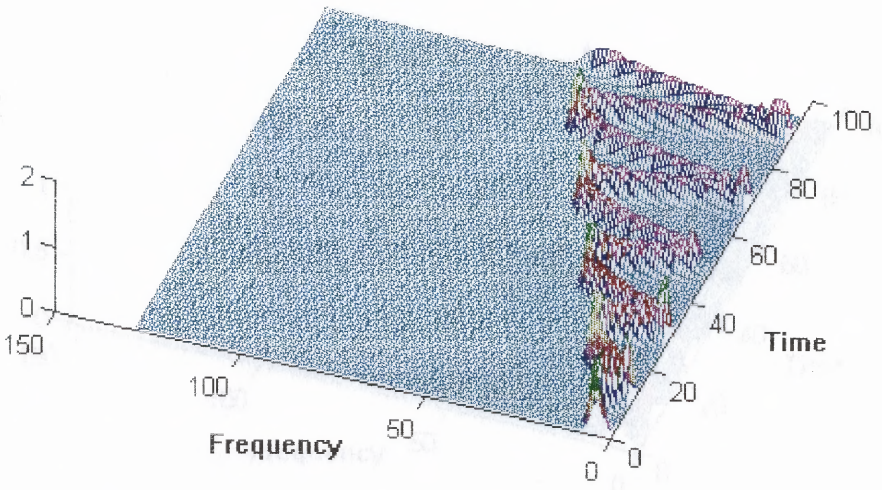

Figure 3.5 Time Frequency Distributions of a sine wave with sinusoidally varying frequency: a) STFT

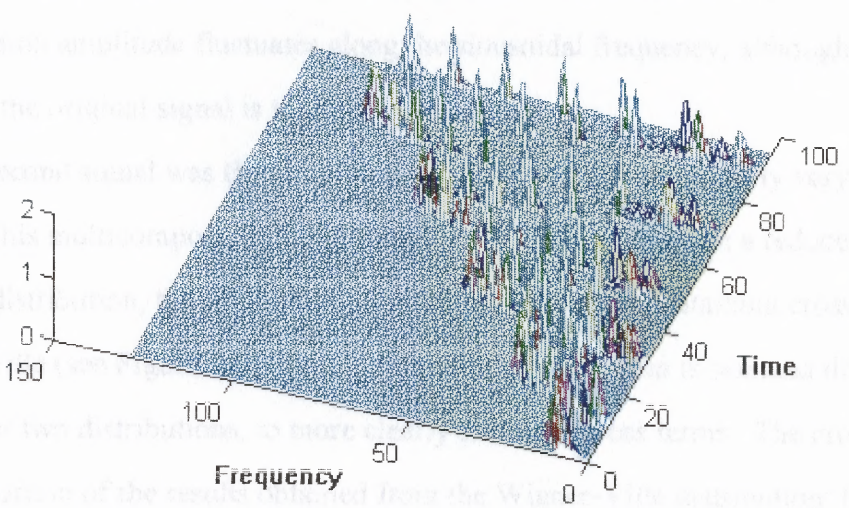

Figure 3.5 Time Frequency Distributions of a sine wave with sinusoidally varying frequency: b) Wigner-Ville

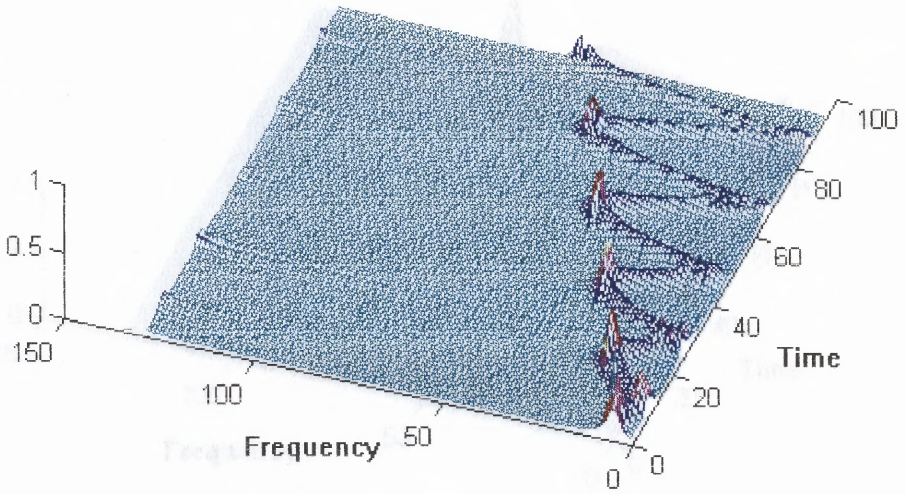

Figure 3.5 Time Frequency Distributions of a sine wave with sinusoidally varying frequency: c) Choi-Williams

The three time frequency distributions' shapes showed the expected pattern. However, the STFT had a wider spectrum than the Choi-Williams and Wigner-Ville. The Wigner-Ville distribution amplitude fluctuates along the sinusoidal frequency, although the amplitude of the original signal is the same throughout.

The second signal was the chirp plus a sine wave with sinusoidally varying frequency. This multicomponent signal shows the difference between a reduced interference distribution, the Choi-Williams, and a distribution containing cross terms, the Wigner-Ville (see Figure 3.6). The Wigner-Ville distribution is oriented differently from the other two distributions, to more clearly show the cross terms. The cross terms are a major portion of the results obtained from the Wigner-Ville distribution; therefore, when the Wigner-Ville is applied to the EMG data, incorrect results can be expected.

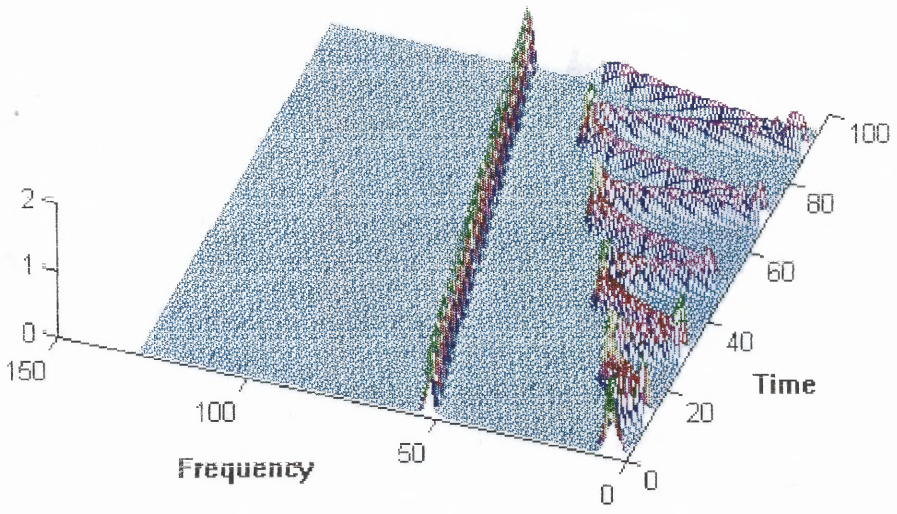

Figure 3.6 Time Frequency distributions of a multicomponent signal: a) STFT

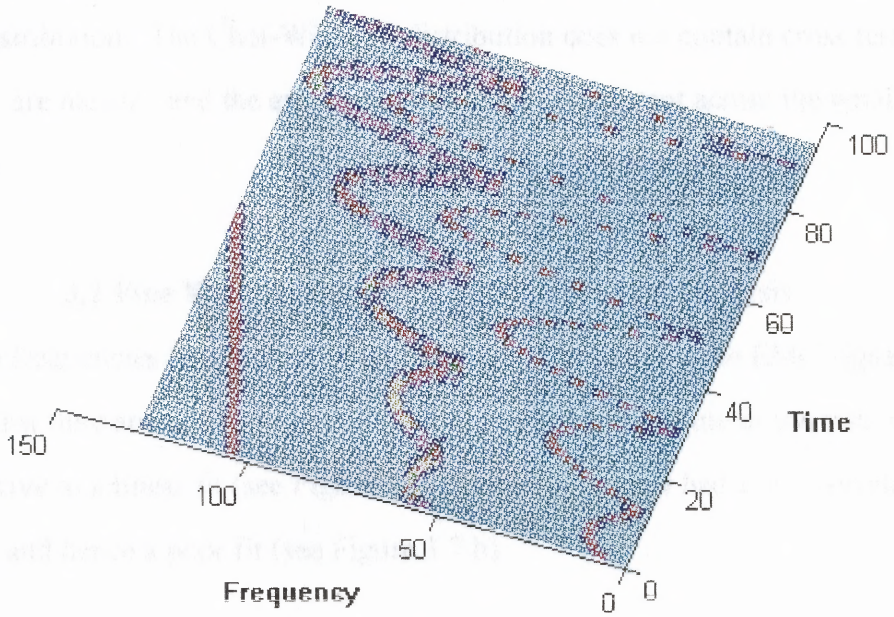

Figure 3.6 Time Frequency distributions of a multicomponent signal: b) Wigner-Ville

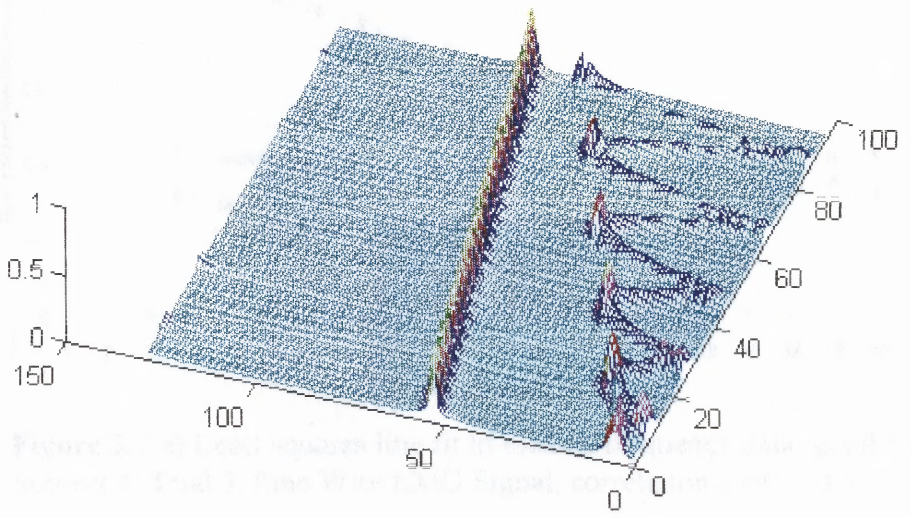

Figure 3.6 Time Frequency distributions of a multicomponent signal: c) Choi-Williams

The results obtained from both test signals, indicate that the Choi-Williams is the preferred distribution. The Choi-Williams distribution does not contain cross terms, the components are narrow, and the amplitude is basically consistent across the whole distribution.

3.2 Fine Wire versus Surface EMG Spectral Analysis

The median frequencies obtained from both the fine wire and surface EMG signals were plotted against time and a linear least squares fit was applied. Some of the tests were very conducive to a linear fit (see Figure 3.7 a), while other test had a low correlation coefficient, and hence a poor fit (see Figure 3.7 b).

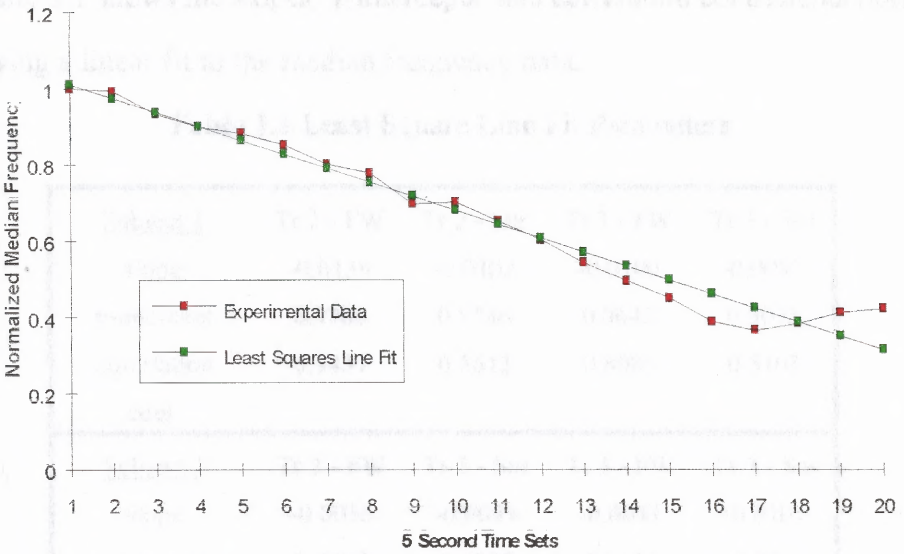

Figure 3.7 a) Least squares line fit to median frequency data: good fit Subject 4, Trial 3, Fine Wire EMG Signal, correlation coef. = 0.97

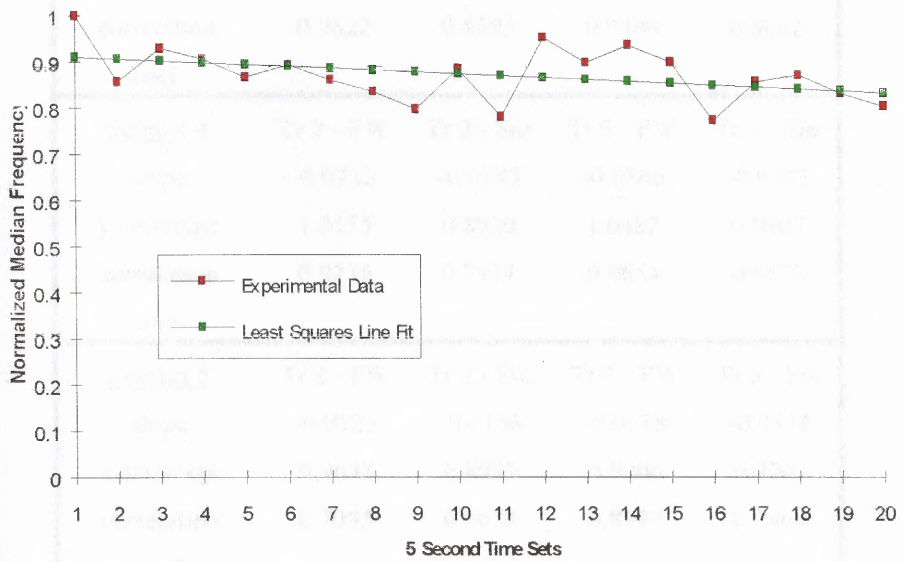

Figure 3.7 b) Least squares line fit to median frequency data: poor fit Subject 2, Trial 3, Fine Wire EMG Signal, correlation coef. = 0.17

Table 3.1 shows the slopes, y-intercepts, and correlation coefficients obtained after applying a linear fit to the median frequency data.

Table 3.1 Least Square Line Fit Parameters

Subject 1	Tr 2 - FW	Tr 2 - Sur	Tr 3 - FW	Tr 3 - Sur
slope	-0.0139	-0.0102	-0.0100	-0.0097
y-intercept	0.9706	0.9746	0.9643	0.9075
correlation coef.	0.9451	0.5612	0.8085	0.5103
Subject 2	Tr 2 - FW	Tr 2 - Sur	Tr 3 - FW	Tr 3 - Sur
slope	-0.0058	-0.0049	-0.0041	-0.0107
y-intercept	0.9305	0.9289	0.9145	1.010
correlation coef.	0.2245	0.2244	0.1726	0.7189
Subject 3	Tr 2 - FW	Tr 2 - Sur	Tr 3 - FW	Tr 3 - Sur
slope	-0.0257	-0.0180	-0.0240	-0.0193
y-intercept	0.9953	0.9271	0.9670	0.9151
correlation coef.	0.9622	0.8395	0.9488	0.9002
Subject 4	Tr 2 - FW	Tr 2 - Sur	Tr 3 - FW	Tr 3 - Sur
slope	-0.0232	-0.0193	-0.0366	-0.0333
y-intercept	1.0155	0.8920	1.0482	0.9907
correlation coef.	0.9235	0.7914	0.9654	0.9573
Subject 5	Tr 2 - FW	Tr 2 - Sur	Tr 3 - FW	Tr 3 - Sur
slope	-0.0123	-0.0156	-0.0158	-0.0134
y-intercept	0.9635	0.8937	0.9306	0.9701
correlation coef.	0.7095	0.5674	0.8977	0.7466

Except for the second trial of subject 5, the slope of the median frequency versus contraction time was greater for the fine wire signal than for the surface signal. For two of the subjects, the slopes were greater for the third trial (for both fine wire and surface

data) than for the second, but the opposite was true for the other 3 subjects. This is not a definitive study on the effectiveness of using the median frequency of fine wire EMG signal to measure fatigue. The results appear to show, however, that median frequency of the fine wire EMG signal decreases with more with fatigue than the median frequency of the surface EMG signal.

3.3 Time Frequency Analysis

3.3.1 Fine Wire EMG Signal

The three time frequency distributions were applied to the fine wire EMG signal. The results for subject 1, trial 3 are shown in Figures 3.8, 3.9, and 3.10.

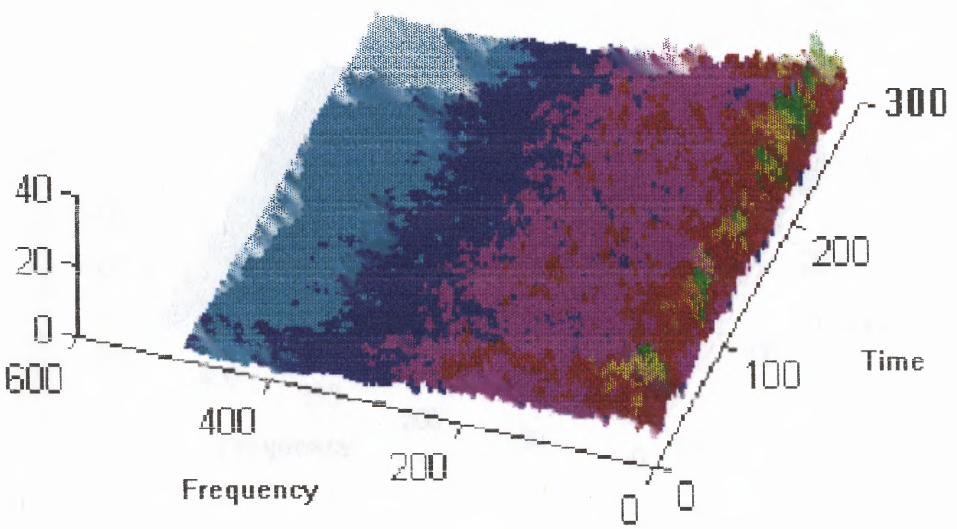

Figure 3.8 Time Frequency Distribution - Fine Wire EMG signal: STFT

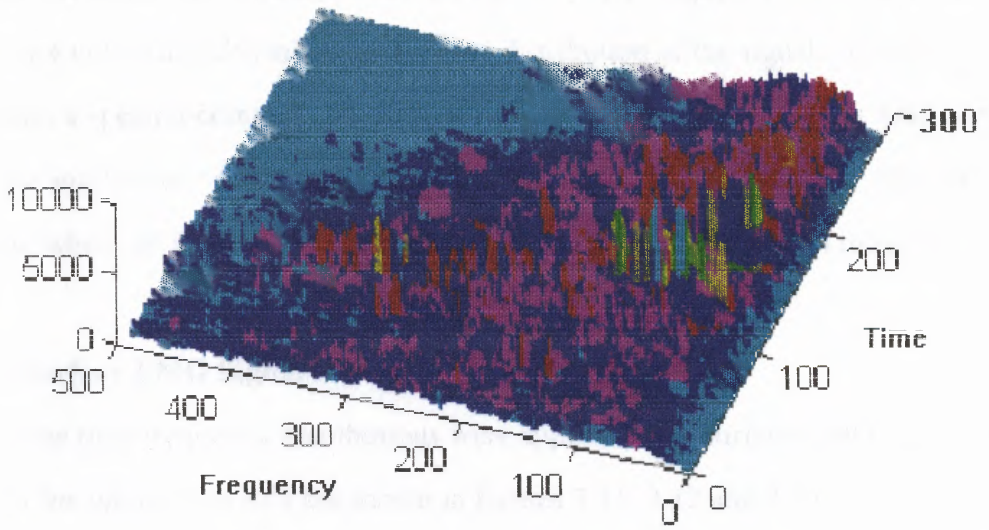

Figure 3.9 Time Frequency Distribution - Fine Wire EMG signal: Wigner-Ville

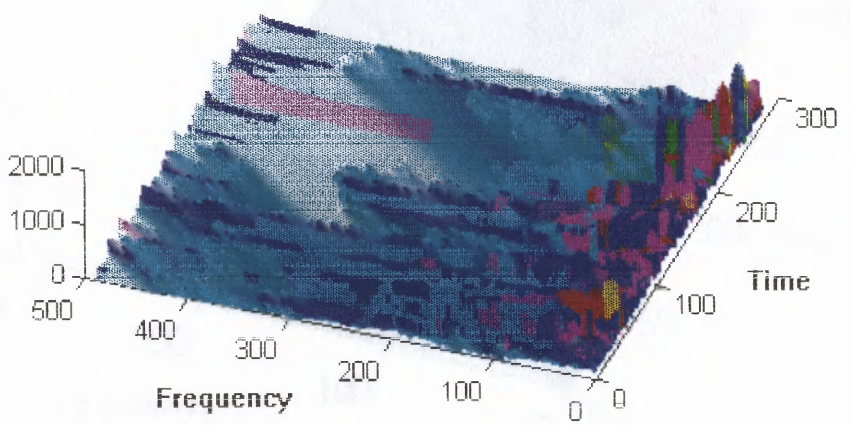

Figure 3.10 Time Frequency Distribution - Fine Wire EMG Signal - Choi-Williams

The three time frequency distributions produce very different distributions. The STFT distribution has very wide spectrum components, and the only indication of spectral compression is a slight rise in amplitude at the end of the contraction. The Wigner-Ville distribution most clearly shows the spectral compression. At the beginning of that distribution the frequency components extend across the entire frequency domain,

as time increases the distribution narrows to the lower frequency end. However the cross terms are not distinguishable from the true distribution of the signal. The Choi-Williams indicates a spectral compression because the frequency spread is less as time increases and the amplitudes of the spectrum are higher at the lower frequencies. The walls, points in time where all frequencies exist, make this distribution difficult to intrepret.

3.3.2 Surface EMG Signal

The three time frequency distributions were applied to the surface EMG signal. The results for subject 1, trial 3 are shown in figures 3.11, 3.12 and 3.13.

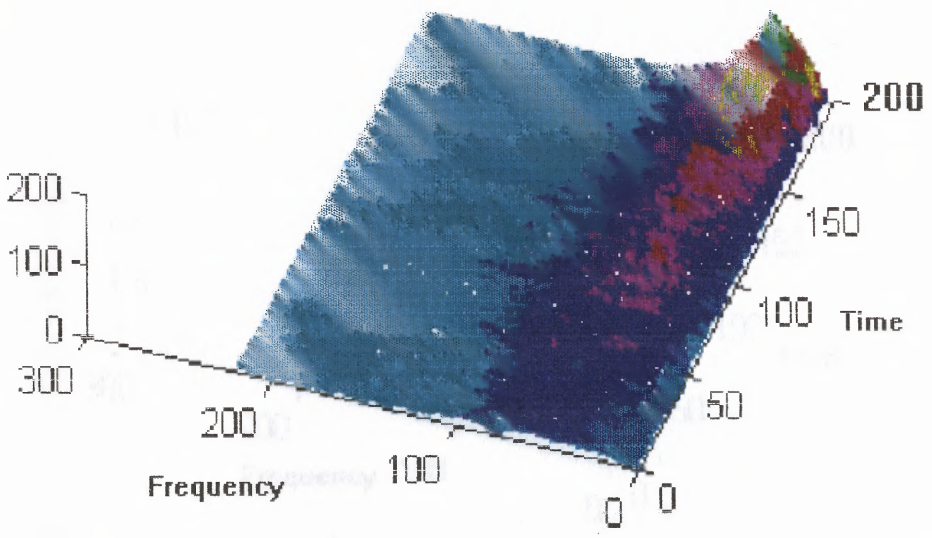

Figure 3.11 Time Frequency Distribution - Surface EMG signal: STFT

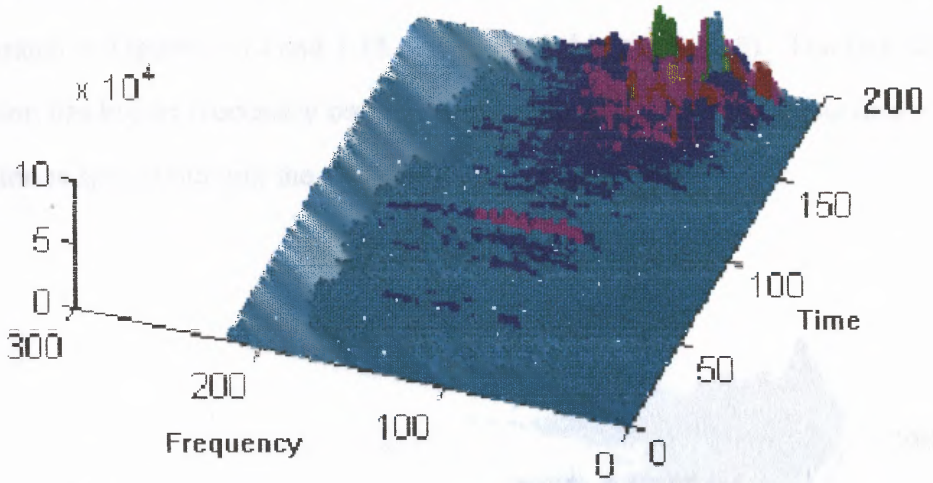

Figure 3.12 Time Frequency Distribution - Surface EMG signal: Wigner-Ville

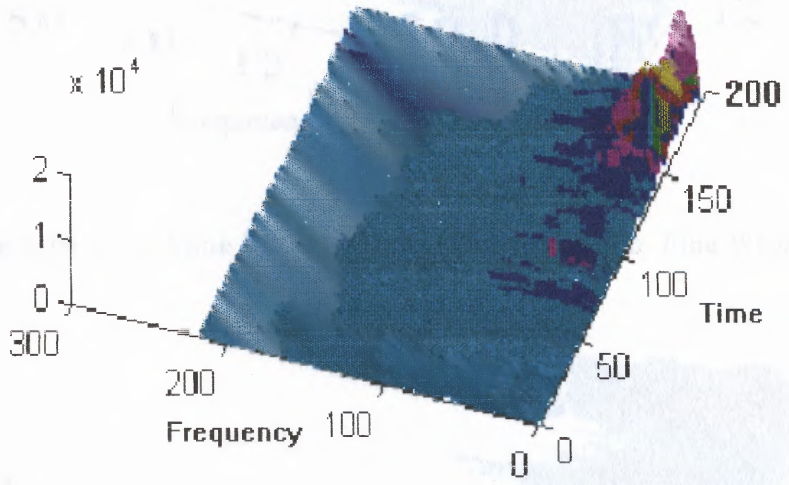

Figure 3.13 Time Frequency Distribution - Surface EMG signal: Choi-Williams

The spectral compression is clearly seen in all three distributions. However, less of the distribution is seen at earlier times with the Wigner-Ville and Choi-Williams. Again, as with the fine wire data, the STFT distribution is more spread out over frequency.

3.3.3 Short Time Fourier Transform

The differences between the STFT distribution for fine wire signal and the surface signal are illustrated in Figures 3.14 and 3.15 (data from subject 3, trial 2). The fine wire distribution has higher frequency components, which is expected. The surface distribution is spread out and the compression is difficult to see.

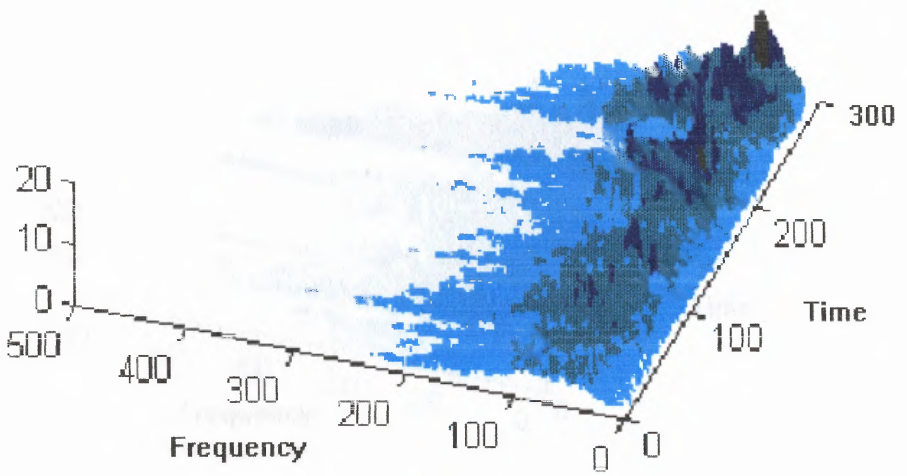

Figure 3.14 Short Time Fourier Transform Distribution: Fine Wire EMG signal

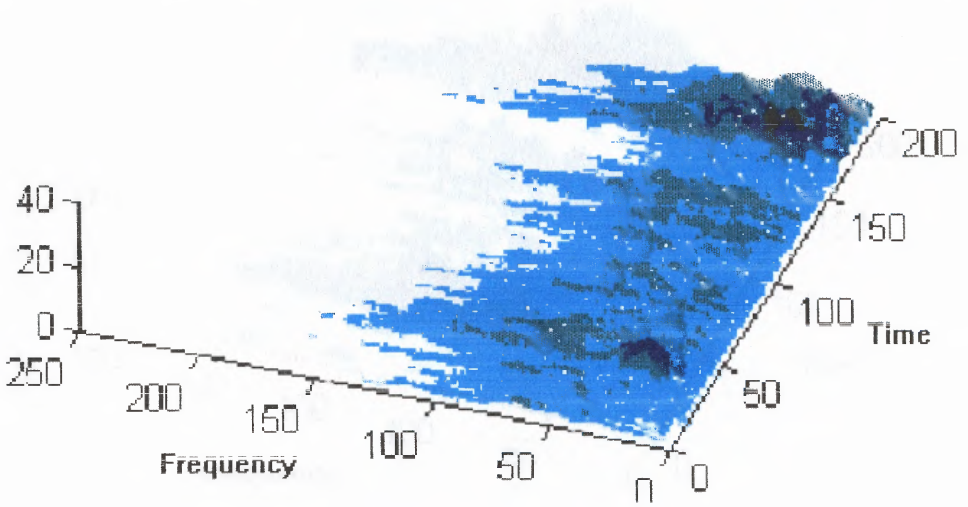

Figure 3.15 Short Time Fourier Transform Distribution: Surface EMG signal

3.3.4 Wigner-Ville Distribution

The differences between the Wigner-Ville distribution for the fine wire signal and the surface signal are illustrated in Figures 3.16 and 3.17 (data from subject 3, trial 2). Again, as with the STFT, the fine wire distribution has higher frequency components. However, neither the surface or the fine wire distribution indicate spectral compression clearly.

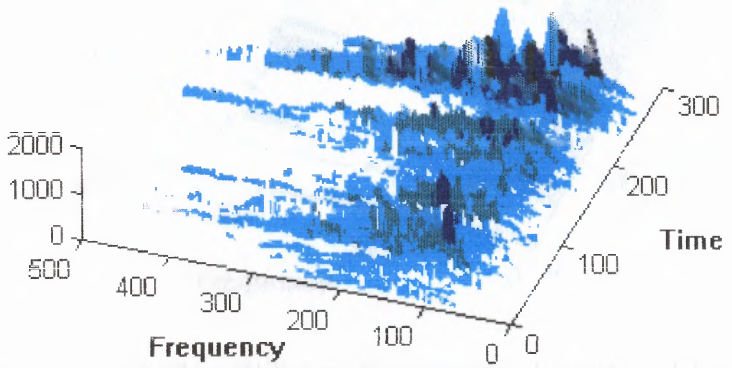

Figure 3.16 Wigner-Ville Distribution: Fine Wire EMG signal

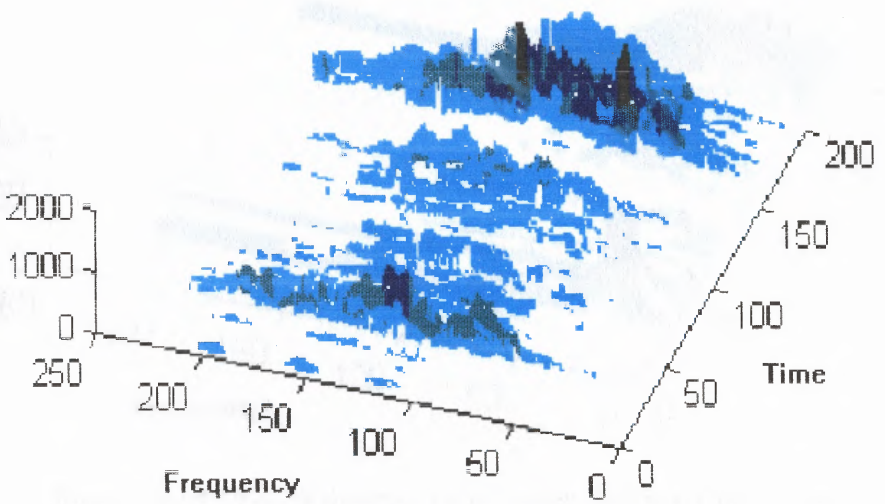

Figure 3.17 Wigner-Ville Distribution: Surface EMG signal

3.3.5 Choi-Williams Distribution

The differences between the Choi-Williams distribution for the fine wire signal and the surface signal are illustrated in Figures 3.18 and 3.19 (data from subject 3, trial 2). The Choi-Williams distribution is the most similar for both fine wire and surface signals. The walls in the surface distribution are less distinct than those in the fine wire distribution.

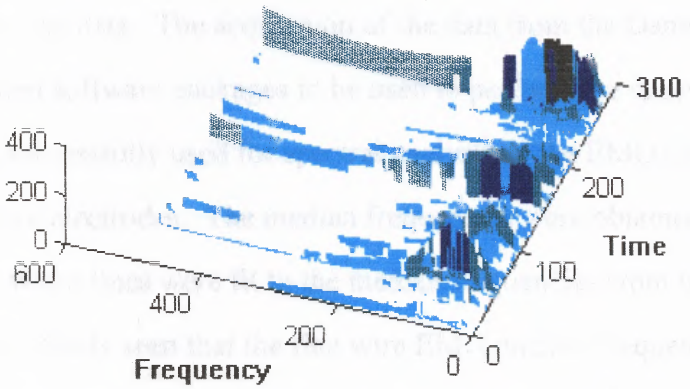

Figure 3.18 Choi-Williams Distribution: Fine Wire EMG signal

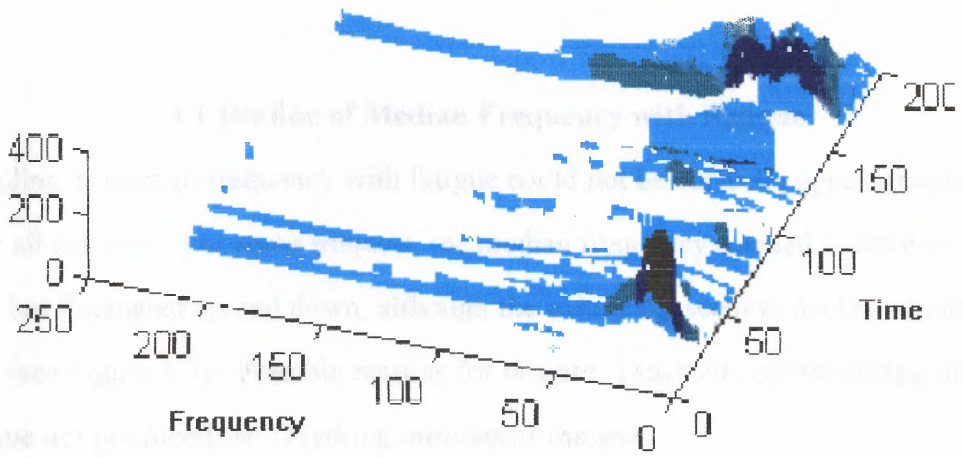

Figure 3.19 Choi-Williams Distribution: Surface EMG signal

CHAPTER 4

DISCUSSION AND CONCLUSIONS

The setup for data acquisition was computerized, allowing the simultaneous acquisition of two channels of EMG data. The setup was automated, so no engineering knowledge is necessary to collect the data. The acquisition of the data from the Dantec Counterpoint enabled sophisticated software packages to be used to perform the spectral analysis.

SPlus was successfully used for spectral analysis of the EMG signal from both the fine wire and surface electrodes. The median frequencies were obtained across the contraction time. When lines were fit to the median frequencies from the fine wire and surface data, it was clearly seen that the fine wire EMG median frequency decreased with fatigue in the same manner as the surface EMG median frequency.

A first attempt was made at applying time frequency techniques to the EMG signal during fatigue. In general, the results were good, showing the expected spectral compression with time of contraction.

4.1 Decline of Median Frequency with Fatigue

The decline of median frequency with fatigue could not be correctly approximated by a line for all subjects. For some subjects, the median frequency seemed to have no definite pattern but fluctuated up and down, although the values did seem to decline slightly overall (see Figure 3.7). Possible reasons for this are: 1) activity of synergistic muscles; 2) fatigue not produced; or 3) jerking motions of the arm.

Duchêne and Goubel (1990) investigated the effect of synergistic muscle activity on the spectral parameters of the EMG signal. They found that when there were alternations in the activity between synergistic muscles, there were large variations in the spectral parameters. Due to these large variations, a single spectral parameter, like the

median frequency, was not a valid indicator of fatigue (Duchêne and Goubel, 1990).

Although the weight chosen for each subject was assumed adequate to produce fatigue, some subjects did not experience any psychological fatigue and therefore may not have experienced any physiological fatigue. The subjects whose median frequencies fluctuated up and down the most were the subjects who had very little decline in median frequency, indicating little physiological fatigue.

The subjects were requested to hold their arms at the required 45° angle. As the biceps muscle fatigued, some of the subjects dropped their arm slightly. When told they were doing this, they would jerk their arm up. This movement lengthened and then quickly shortened the contraction moment arm, which would affect the amount of force needed and the median frequency.

4.2 Data Acquisition

The filters on the Dantec Counterpoint were assumed adequate to filter both DC signals and signals with frequencies above 2000 Hertz. However, the spectrum contained values at zero frequency and frequencies above 2000 Hertz. Values at these frequencies could be eliminated by adding external analog filters between the Counterpoint and the data acquisition computer. To further improve the design, the filters should be different for the surface EMG signal and the fine wire EMG signal. Since frequencies above 200 Hertz are not expected for the surface EMG signal, a low-pass filter with a cut-off frequency of 200 Hertz should be designed for this channel. Fine wire EMG signals can contain frequencies as high as 1000 Hertz, so a low-pass filter with a cut-off of 1000 Hertz should be incorporated into the design. Both signals should have frequencies below 20 Hertz filtered out.

4.3 Time Frequency Analysis

The Short Time Fourier Transform, STFT, distribution appears to most clearly show the compression of the spectrum as the muscle fatigues. However, the STFT does not satisfy the marginal properties. This factor implies that when a time slice of the STFT distribution is taken, it does not equal the power density spectrum at that point in time. The same is true for a frequency slice of the distribution. The STFT also does not satisfy properties 9 and 10, time and frequency support. The time support property is not satisfied because the distribution is not necessarily zero before or after the signal or at any time when the signal is zero. If the original signal is bandlimited, the STFT distribution may not be zero outside the band; therefore the frequency support property is not satisfied. Because four of the eleven desired properties are not satisfied, the STFT is not a reliable representation of the frequency changes through time of the EMG signal.

The Wigner-Ville distribution intrinsically has cross-terms and therefore is not a precise representation of the changing of the frequency components with fatigue. The Wigner-Ville distribution also offsets the frequency components of the signal. This is not reported anywhere in the literature, so it may be a result of a problem in the programming.

The joint time-frequency densities obtained using the Choi-Williams distribution seem to most accurately show the frequency compression. The walls in the distribution (points in time when it appears that all frequencies exist) make this distribution hard to analyze. One reason for this wall is illustrated in Figure 4.1.

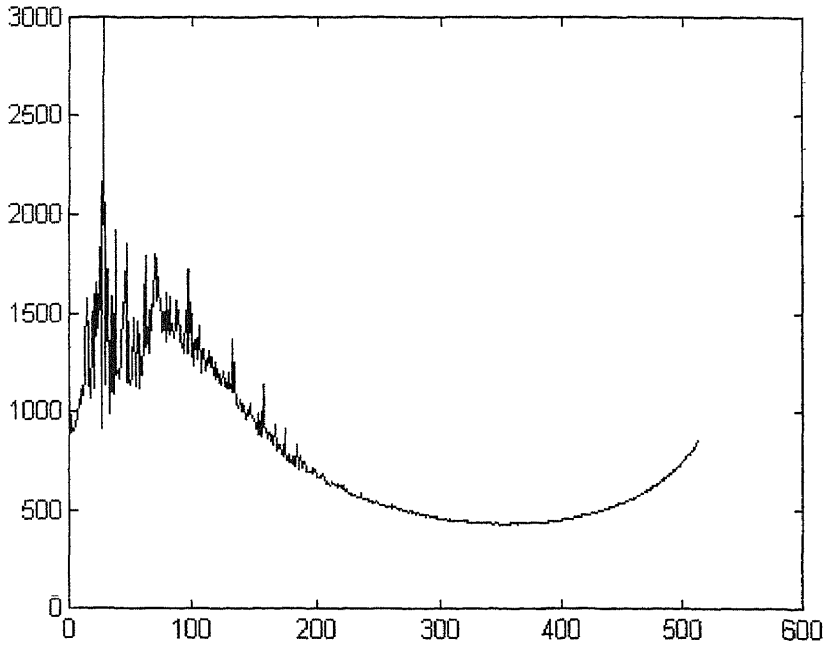

Figure 4.1 Walls in Choi-Williams Distributions:
a) time slice of distribution where wall appears

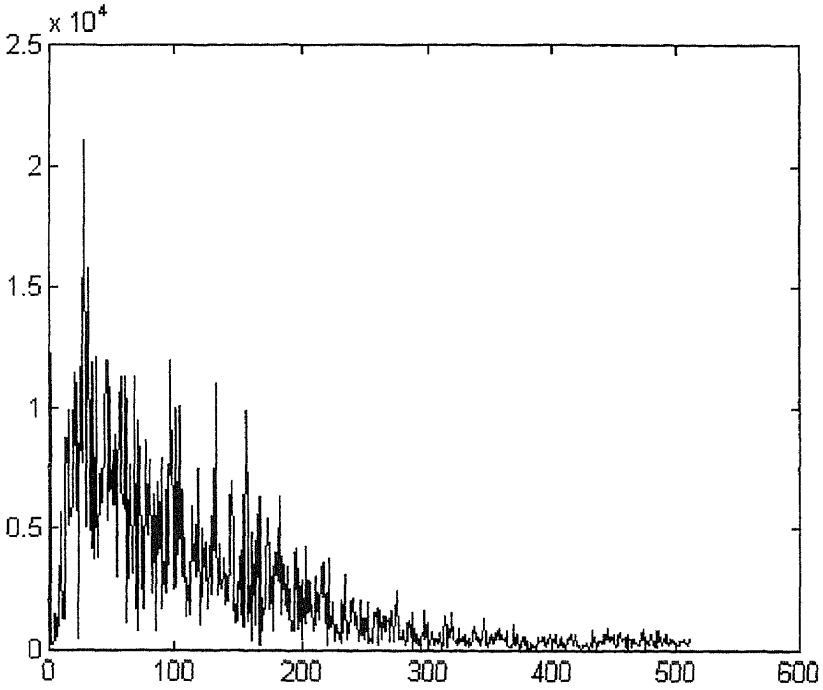

Figure 4.1 Walls in Choi-Williams Distributions:
b) traditional fft of original signal at that same time

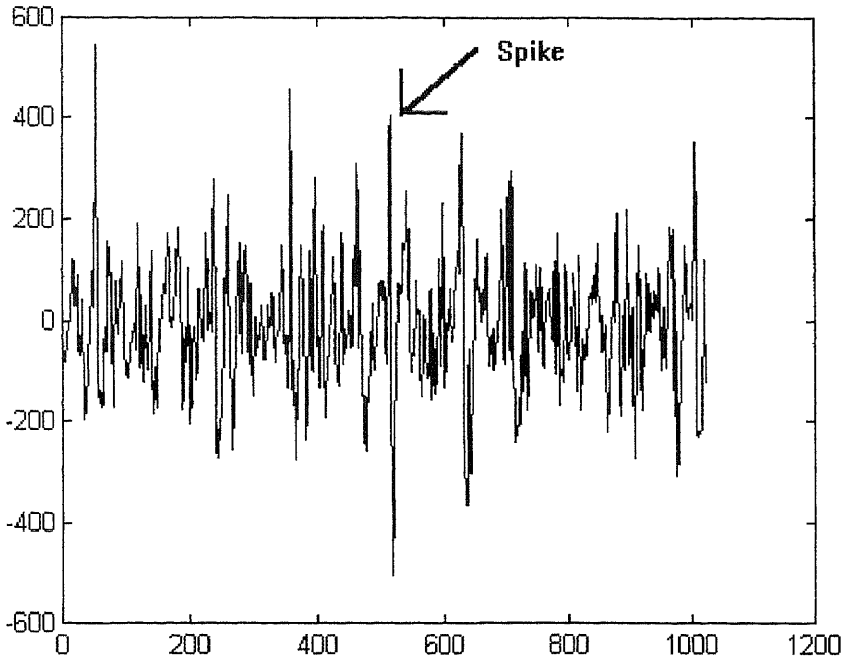

Figure 4.1 Walls in Choi-Williams Distributions:
c) the original EMG signal at that point in time.

At the time when the wall appears in the Choi-Williams distribution, the original EMG signal shows a spike. The Fourier Transform of a spike is a straight line including all frequencies. When there is a spike in the original signal, the spectrum should contain all frequencies. Since the Choi-Williams is the only one of the three time frequency distributions used here that contains this spectrum for the spike, it would seem to the most accurate distribution. However, it is not clear that spikes in the original EMG signal are significant in the study of muscle fatigue and the compression of the spectrum with that fatigue. If the spikes are found not to be significant, it would suggest that the walls are a hindrance to the analysis of the Choi-Williams distribution. The distributions were smoothed across 12 points in frequency, but no smoothing was done across the time axis. Smoothing there could possibly decrease the effects of the walls.

CHAPTER 5

SUGGESTIONS FOR THE FUTURE

5.1 Data Collection

There were many variables in the experimental set-up that may have caused deviations in the spectral analysis of both the fine wire and surface EMG signal. Some of these parameters are: position of electrodes, position of arm, and choice of weight. The midway point between the muscle peak and the tendon was measured and recorded. This measurement insured that the fine wire electrode was inserted at the same point for the two days the subject was tested. The depth the fine wire electrode was inserted into the muscle was not recorded, so from the first testing date to the next, the electrode could have been measuring different motor units. Also, the surface electrode was placed next to the fine wire electrode but was placed distal, medial or lateral depending on the subject tested. The location of the surface electrode in comparison with the fine wire electrode could influence the amount of correlation between the spectral parameters of the two signals.

The arm was positioned at a 45° angle, but this angle was not measured exactly, so it was not precise. There was no method for maintaining this position. Changing the position affected the moment arm, which changed the amount of force required to maintain the contraction. The change in force caused a change in the EMG signal which affected the spectral parameters. A goniometer should be used to accurately measure the position of the arm, and a way should be found for the subject to maintain that position.

The MVC was found using a Cybex pulley system, while the experiment was performed with a dumbbell. It can not be assumed that 30% of the MVC found using the Cybex is the correct weight to be used for an experiment using dumbbells because the Cybex uses a pulley system which decreases the amount of force needed.

5.2 Time Frequency Analysis

This is the first time time frequency techniques have been applied to the EMG signal and the first time these techniques were used at Kessler Institute for Rehabilitation. The first time a new technique is used, many questions arise. Some have been answered, but many more need to be answered to obtain a fuller understanding of this technique.

Time frequency techniques can be very sensitive to fluctuations in the signal, as was shown by the walls in the Choi-Williams distributions. If the fluctuations do not contain pertinent information for the study, they should be filtered out. Time frequency techniques require a very clean signal.

When applying a time frequency technique, there are three parameters that need to be set up: the number of time slices, the size of the FFT, and the number of points to skip between the beginning of each FFT. The number of points to skip multiplied by the number of time slices is approximately the number of points in the original signal. To obtain the optimum value, experiments should be done varying the number of points skipped for the type of signal to be studied. Also, the size of the FFT should be varied depending on the type of signal to be analyzed.

The kernel distribution program is very time consuming. With the Choi-Williams kernel, it took over one hour to analyze 200,000 points of data (a 100 second contraction) on a 50 MHz, 486dx computer. This program should be modified to be more time efficient.

The graphing methods available in Matlab are very sensitive to amplitude. From the time frequency plots in Chapter 3, it would appear that at the beginning of the contraction, the spectrum is the constant across all frequencies. This is not the case, but it appears this way because the amplitude here is very small compared to the amplitude of the spectrum at the end of the contraction. Different graphing techniques need to be investigated to find one that most clearly shows the spectra across all time slices. One possibility is to use the log of the amplitude.

There are many other time frequency distributions. The STFT and Wigner-Ville distributions were chosen for this project, because they have been used widely in the past. Therefore, there are well understood and can be used as a basis for comparison. The Choi-Williams distribution was arbitarily chosen from a group of reduced interference distributions. Some of the other distributions available are the Born-Jordan, the G-Hamming, the Truncated-CW, the Truncated-Sinc and the Triangular distributions. After some of the previous questions have been addressed, these other time frequency distributions could be applied to the EMG signal. Different distributions will emphasize different properties of the joint time frequency density.

The graphs seen are pictures of the change in frequency components throughout the time of the signal. Nothing has been done to use the actual matrix from which the plots are made. Techniques should be developed to manipulate the data contained in the time frequency matrix. Numerical representations of fatigue , which are more objective than graphical representations, could be extracted from this matrix. These values may provide better estimates of fatigue than the traditional spectral parameters: mean and median frequency. One such numerical representation would be the instantaneous frequency. For every time slice, the instantaneous frequency could be calculated. This value may decrease with spectral compression in a way similar to the median frequency. If that did happen, a relationship would need to be found between the median frequency, obtained with traditional spectral analysis methods, and the instantaneous frequency.

APPENDIX A

Data Acquisition

Before acquiring data from the Dantec Counterpoint, the data acquisition had to be set up with files for data storage. Streamer's make file command (MKFILE) was used to create the data storage files with the appropriate size. The size of the file was calculated using the sampling rate per channel (SR), the total sampling time (t), and the number of channels to be acquired (CH).

$$size = \frac{SR * CH * t * 2}{1000} \tag{A.1}$$

The sampling rate chosen was two times the highest frequency expected. The highest frequency was estimated to be 2000 Hertz, so a sampling rate of 4000 Hertz per channel was used. Each file stored the data from one 100-second trial, indicating a 100-second sampling time.

$$size = \frac{4000 * 2 * 100 * 2}{1000} = 1600 \tag{A.2}$$

Each data file was unpacked into 20 ASCII files, each of which contained five seconds of the trial. A batch file was written to unpack all 20 files at one time. The first line was: unpack %1.dat,%1.1,0-39999/b/das16, while the last line was unpack 1.dat,%1.20, 760000-799999/b/das16. An example of this batch file is:

```
munpack datafile

unpack datafile.dat, datafile.1,0-39999/b/das16
unpack datafile.dat, datafile.20,760000-799999/b/das16.
```

APPENDIX B

SPLUS PROGRAMMING DETAILS

1. Each file was scanned into SPlus,where the spectral analysis took place.

   m928a1_matrix(scan("m928a.1",skip=1,sep=","),ncol=2,byrow=T)

2. The FFT of each channel was then taken.

   m928a1.f1_FFT(m928a1[,1]

   m928a1.f2_FFT(m928a1[,2]

3. After the FFT was computed, the median frequency of the FFT was calculated. The following program was written for this project to calculate the median frequency.

```
Medfrq2
function (filename)
        {tot_filename * c(1:length(filename))
        desired_sum(tot)/2
        cumul_signif (cumsum(tot),digits = 4)
        medfreq1_match(signif(desired,digits= 4),cumul)
        digs_4
        if (medfreq1 = = "NA")
                {cumul_signif (cumsum(tot),digits = 3)
                medfreq1_match(signif(desired,digits= 3),cumul)
                digs_3}
        if (medfreq1 = = "NA")
                {cumul_signif (cumsum(tot),digits = 2)
                medfreq1_match(signif(desired,digits= 2),cumul)
                digs_2}
        medfreq_list (digits = digs, med = medfreq1)
        medfreq}
```

This program calculated the sum of all the amplitudes multiplied by the frequencies at which they occured. (The frequency in SPus was actually just an index number. It was not converted to Hertz until the Excel program.) The program then searched for half of that sum by calculating a running cumulative sum of the amplitude times the frequency. When the cumulative sum that was closest to half the total value was found, that index point was the median frequency. An exact match could not be found, so the program looked first for a match of four significant figures. If a match of four significant figures could not be found, the program searched for three and then two significant figures. The significant figure used for each value was noted, so the values that matched by only two significant figures could be hand checked. The values matched by only two significant figures were off by a maximum of 15 index points, which corresponded to 2.5 hertz.

Frequencies below 20 hertz are unpredictable (DeLuca, 1993), and therefore, this calculation began at 20 hertz instead of zero. For the calculation on the fine wire signal, the indices that corresponded to the values between 2.5 hertz above and below 60 hertz were set to zero for the fine wire calculation, to remove noise 60 hertz noise.

Although the mean frequency was not used in the final results of this experiment. It was used preliminary. The program written to calculate mean frequency is as follows:

```
mnfrq_function(filename)
        {tot_filename*c(1:length(filename)) %calculate A_i times f_i
        mnfreq_sum(tot)/sum(filename)       %mean=sum(tot)/sum(A_i)
mnfrq}
```

APPENDIX C

TIME FREQUENCY DISTRIBUTIONS

Short Time Fourier Transform

The STFT and Wigner-Ville programs, written in Matlab, were obtained from another source, but were slightly modified to allow the input of variables: k, m, and skip.

```
% requires x (original signal)
k = input ('Please enter the number of spectra to be computed ');
m = input ('Please enter the size of the FFT to be computed ');
skip = input ('Please enter the number of points to skip ');
index = 1:m;
p = m/2+1;              % number of frequency values computed
KMU = 4/m;
Z = zeros(p,k);         % initialize result matrix
for i = 1:k
        xw=w'.*(x(index));
        Xx=abs(FFT(xw,m));
        X=KMU*Xx(1:p);
        Z(:,i) = X';    % first time slice of result matrix
        index = index + skip   % moving to next starting point for FFT
end
mesh(Z)
```

Wigner-Ville Distribution

```
% requires x (original signal)
k = input ('Please enter the number of spectra to be computed ');
m = input ('Please enter the size of the FFT to be computed ') ;
```

```
skip = input ('Please enter the number of points to skip ');
w = hanning (m)';       % make hanning window
xh = hilbert(x);        % forms the analytic function of x
L = m/2;
p = m/2+1;      % the number of freq values to be plotted
l = -(L-1):(L-1);
Z = zeros(p,k);         % initialize result matrix
n = L;
for i = 1:k
        g = x(n+l).*conj(x(n-l));
        g(2*L) = 0;
        y = w.*g;       % Apply window to g
        Y = 2/m*abs(FFT(y);
        Z(:,i) = Y(1:p)';       % first time slice of result matrix
        n = n+skip;
end
mesh(Z)
```

Kernel Distribution Program

The kernel distribtuion program was not available and had to be written, along with the program to calculated the Choi-Williams kernel.

```
% requires x (original signal) and g (Fourier transform of kernel to be used)
k = input ('Please enter the number of spectra to be computed ');
sz = input ('Please enter the size of the FFT to be computed ');
skip = input ('Please enter the number of points to be skipped ');
xh=x';
xh=hilbert(xh);  % forms the analytic function of x
```

```
L=sz/2;
n=sz+1;
for i=1:k;      % time shifting
    for m=0:L;      %frequency shifting and convolution with kernel
        p=1:L;
        r2(1)=g(1,m+1)*xh(n+m)*conj(xh(n-m));
        r2(p+1)=g(p+1,m+1).*(xh(p+n+m).*conj(xh(p+n-m))+
                xh(-p+n+m).*conj(xh(-p+n-m)));
        r(m+1)=sum(r2);
    end
    Y=2/m*abs(FFT(r));
    Z(:,i)=Y(1:(L+1)';   %sets first column of Z equal to first FFT
    n=n+skip;
end
mesh(Z)
```

Choi-Williams Kernel

```
%           Choi-Williams Distribution Specification Matrix
%  Values for sigma and the size of G are user inputs.
hlf = input('please enter half the size of the FFT ')
o=input('please enter the value for sigma ')
g(hlf+1,hlf+1)=0;
g(1,1)=1;
wt=0;
for b=1:hlf
    a=0:hlf;
    g(a+1,b+1)=exp(-(o*a.^2)/(4*b^2))';
```

```
end
b=1:hlf
 wt(b+1)=2*sum(g(:,b+1))-g(1,b+1);
for b=2:hlf+1
      g(:,b)=g(:,b)/wt(b);
end
g;
```

REFERENCES

Amin, M., L. Cohen, and W.J. Williams. 1993. "Methods and Applications for Time Frequency Analysis". Conference Notes, University of Michigan.

Badier M., C. Guillor, F. Lagier-Tessonnier, H. Burnet, and Y. Jammes. 1993. "EMG Power Spectrum of Respiratory and Skeletal Msucles During Static Contraction in Healthy Man." *Muscle and Nerve.* 6:601-609.

Basmajian J.V., and C.J. DeLuca. 1985. Muscles Alive. John Butler. Fifth Edition. Baltimore: Williams & Wilkins.

Castaldo, R., E. Quarto, and F. Clemente. 1991. "A Real-Time FFT Analyser for Monitoring Muscle Fatigue." *Journal of Biomedical Engineering.* 13:465-468.

Cromwell, L., F.J. Weibell, and E.A. Pfeiffer. 1980. "The Nervous System." *Biomedical Instrumentation & Measurements.* Second Edition. New Jersey: Prentice Hall, Inc. 300-303.

Daanen H.A.M., M. Mazure, M. Holewijn, and E.A. Van der Velde. 1990. "Reproduciblity of the Mean Power Frequency of the Surface Electromyogram." *European Journal of Applied Physiology.* 61:274-277.

Delagi E.F., J Iaezetti. 1981. Anatomic Guide for the Electromyographer: The Limbs. Springfield: Charles C. Thomas. 66-67.

DeLuca C.J., M.A. Sabbahi, F.B. Stulen and G. Bilotto. 1983. "Some Properties of the Median Frequency of the Myoelectric Signal during Localized Muscular Fatigue." *Proceeding of the 5th International Symposium of the Biochemistiry of Exercise. Human Kinetic Publishers, Chicago.* 175-186.

DeLuca C.J. 1993. Personal Communication

Duchêne, J. and F. Goubel. 1990. "EMG Spectral Shift as an Indicator of Fatigability in a Heterogeneous Muscle Group." *European Journal of Applied Physiology.* 61:81-87.

Hägg, G.M. 1991. "Comparison of Different Estimators of Electromyographic Spectral Shifts During Work When Applied on Short Test Contractions." *Medical and Biological Engineering and Computing.* 29:511-516.

Knaflitz, M., and B. Gabriella. 1991. "Computer Analysis of the Myoelectric Signal." *IEEE Micro.* 10:12-15,48-58

REFERENCES
(Continued)

Krogh-Lund C. and K. Jørgensen. 1993. "Myo-electric Fatigue Manifestations Revisited: Power Spectrum, Conduction Velocity, and Amplitude of Human Elbow Flexor Muscles During Isolated and Repetitive Endurance Contraction at 30% Maximal Voluntary Contraction." *European Journal of Applied Physiology.* 66:161-173.

Linssen, W.H.J.P., D.F. Stegeman, E.M.G. Joosten, M.A. van't Hof, R.A. Binkhorst, and S.L.H. Notermans. 1993. "Variability and Interrelationship of Surface EMG Parameters During Local Muscle Fatigue." *Muscle & Nerve.*16:849-856.

Marieb, E.N. 1992. "Muscles and Muscle Tissue." Human Anatomy and Physiology. 2nd Edition. California: The Benjamin/Cummings Publishing Company, Inc. 246-269.

Merletti R., and C.J. DeLuca. 1992. "Electrical Evoked Myoelectric Signals." *Critical Reviews in Biomedical Engineering.* 19(4):293-340.

Moritani, T., M. Muro, and A. Nagata. 1986. "Intramuscular and Surface Electromygram Changes during Muscle Fatigue." *Journal of Applied Physiology.* 60:1179-1185.

Nagata, S., A.B. Arsenault, D. Gagnon, G. Smyth, and P.A. Mathieu. 1990. "EMG Power Spectrum as a Measure of Muscular Fatigue at Different Levels of Contraction." *Medical and Biological Engineering and Computing.* 28:374-78.

Roy S.H., C.J. DeLuca, and D. A. Casavant. 1989. "Lumber Muscle Fatigue and Chronic Lower Back Pain." *Spine.* 14:992-1001.

Smyth G. A.B. Arsenault, S. Nagata, D. Gagnon, and P.A. Mathieu. 1990. "Slope of the EMG/Moment Relationship as a Measure of Muscular Fatigue: A Validation Study." *Medical and Biological Engineering and Computing.* 28:379-383.

Stulen, F.B., and C.J. DeLuca. 1981. "Frequency Parameters of the Myoelectric Signal as a Measure of Muscle Conduction Velocity." *IEEE Transactions on Biomedical Engineering.* 28:512-523.

---------. 1982. "Muscle Fatigue Monitor: A Noninvasuve Device for Observing Localized Muscular Fatigue." *IEEE Transactions on Biomedical Engineering.* 29:760-768.

Yaar, I. and L. Niles. 1992. "Muscle Fiber Conduction Velocity and Mean Power Spectrum Frequency in Neuromuscular Disorderd and in Fatigue." *Muscle and Nerve.* 15:780-787.